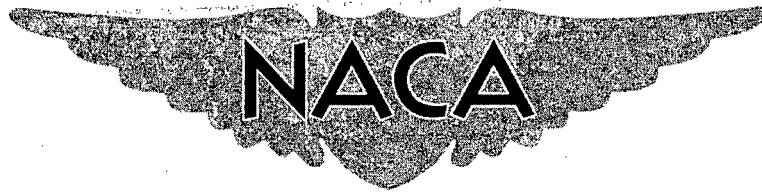


CONFIDENTIAL

Copy 52
RM SL51A03

N-3511
C.2



RESEARCH MEMORANDUM

for the

Bureau of Aeronautics, Department of the Navy

*effective
Apr. 15, 1958*

NACA Re. abn

Date

VEN-126

Am 5-18-58

AN INVESTIGATION OF THE HYDRODYNAMIC CHARACTERISTICS
OF A JET-POWERED DYNAMIC MODEL OF THE
DR 56 FLYING BOAT
TED NO. NACA DE 328

By Arthur W. Carter, Max D. West, and Paul W. Bryce, Jr.

Langley Aeronautical Laboratory
Langley Field, Va.

CLASSIFIED DOCUMENT

This document contains classified information affecting the National Defense of the United States within the meaning of the Espionage Act, USC 50:31 and 32. Its transmission or the revelation of its contents in any manner to an unauthorized person is prohibited by law.

Information so classified may be imparted only to persons in the military and naval services of the United States, appropriate civilian officers and employees of the Federal Government who have a legitimate interest therein, and to United States citizens of known loyalty and discretion who of necessity must be informed thereof.

NATIONAL ADVISORY COMMITTEE FOR AERONAUTICS

WASHINGTON

January 15, 1951

100-2-1-100-100

100-2-1-100-100

CONFIDENTIAL

CLASSIFICATION CHANGED

UNCLASSIFIED

To



NATIONAL ADVISORY COMMITTEE FOR AERONAUTICS

RESEARCH MEMORANDUM

for the

Bureau of Aeronautics, Department of the Navy

AN INVESTIGATION OF THE HYDRODYNAMIC CHARACTERISTICS

OF A JET-POWERED DYNAMIC MODEL OF THE

DR 56 FLYING BOAT

TED NO. NACA DE 328

By Arthur W. Carter, Max D. West, and Paul W. Bryce, Jr.


SUMMARY

An investigation was made of the hydrodynamic characteristics of a $\frac{1}{17}$ -size jet-powered dynamic model of a 130,000-pound transonic flying-boat design having a high length-beam ratio planing-tail hull, sweptback gull wings with integral wing-tip floats, and wing-root jet-power-plant installation. This design is the Bureau of Aeronautics DR 56.

The load-resistance ratio of the hull without the wing was 4.4 at the hump speed. Take-offs were longitudinally stable at all center-of-gravity locations in the normal operating range. Oscillations in trim were obtained at all landing trims in smooth water, but the oscillations damped out rapidly and the landing behavior appeared to be acceptable at landing trims above 12° . Poor directional stability, encountered at high speeds during landings, was improved by use of additional vertical-fin area and a small skeg at the sternpost.

Variations in landing trim from 11° to 20° had a negligible effect on the maximum trim, rise, and vertical and angular accelerations during landings in 8-foot waves. A maximum vertical acceleration of approximately 9g was obtained.

The jet air intakes were clear of spray except at low speeds in short waves. The flaps were heavily wetted over a short speed range.



The tail surfaces were heavily wetted over a wide speed range and might have to be raised to avoid damage in rough water.

INTRODUCTION

Of present importance in the design of high-performance water-based aircraft is the possible influence on the over-all hydrodynamic characteristics of design trends such as jet propulsion and highly loaded swept wings. In order to examine the possibilities and problems associated with such features in a large seaplane, a tank investigation was made of a $\frac{1}{17}$ - size jet-powered dynamic model of a 130,000-pound transonic flying-boat design having sweptback gull wings with integral wing-tip floats and a wing-root jet-power-plant installation. This design study is the Navy Bureau of Aeronautics DR 56 which has a wing loading of 70 pounds per square foot and a potential thrust-weight ratio of 0.4 at a Mach number of 0.9. The hull is a high-length-beam ratio planing-tail type with a gross-load coefficient of 2.8 and operational center-of-gravity positions located, for military purposes, aft of the step.

The investigation of the hydrodynamic qualities of the DR 56 included longitudinal stability during take-off and landing, spray characteristics in the upright and heeled conditions, resistance during take-off in smooth water, and take-off and landing behavior and spray characteristics in waves 8 feet high (full size). Static properties and drifting characteristics also were investigated. The program was intended to provide comprehensive information on typical service operation of the prototype airplane and scaled versions of the basic design.

SYMBOLS

C_{Δ_0}	gross-load coefficient (Δ_0/wb^3)
C_L	aerodynamic-lift coefficient ($\text{Lift}/\frac{1}{2}\rho V^2 S$)
b	maximum beam of hull, feet
b_w	wing span, feet
c	distance from center of buoyancy of tip float to center line of hull, feet

~~CONFIDENTIAL~~

g	acceleration due to gravity (32.2), feet per second per second
h_e	negative metacentric height of seaplane without tip floats, feet
n	normal acceleration, g units
n_v	vertical acceleration, g units
R	resistance, pounds
S	wing area, square feet
V	horizontal velocity, knots
V_v	vertical velocity (sinking speed), feet per minute
w	specific weight of water (63.4 for these tests, usually taken as 64 for sea water), pounds per cubic foot
α	angular acceleration, radians per second per second
γ	flight-path angle, degrees
δ_e	elevator deflection, degrees
δ_f	flap deflection, degrees
Δ_o	gross load, pounds
Δ	load on water, pounds
Δ_t	submerged displacement of tip float, pounds
ϕ_1	angle of heel required to submerge tip float, degrees
ρ	density of air, slugs per cubic foot
τ	trim (angle between forebody keel at step and horizontal), degrees
τ_L	landing trim, degrees

DESCRIPTION OF MODEL AND APPARATUS

Preliminary hull lines and general-arrangement drawings of the DR 56 flying-boat design were furnished by the Bureau of Aeronautics. These hull lines were faired in detail and a $\frac{1}{17}$ -size jet-powered dynamic model was designed* and constructed at the Langley Aeronautical Laboratory. The model was designated Langley tank model 248. Photographs of the model and lines of the hull are shown in figures 1 and 2, respectively. Offsets of the hull are given in table I. The general arrangement of the flying boat is shown in figure 3 and pertinent characteristics and dimensions of the model and full-size airplane are given in table II.

The model was powered with four compressed-air jets, simulating the four jet engines (two in each nacelle) of the full-size airplane. Air was supplied to the model through a flexible rubber hose from four high-pressure air bottles. A regulator valve controlled the flow and pressure of air to the model. Scale thrust and approximately scale inflow were obtained. Slats were attached to the leading edge of the wing in order to delay the stall to an angle of attack approximating that of the full-size airplane. The pitching moment of inertia of the ballasted model was 0.6 slug-foot square.

The investigation was made in Langley tank no. 1, described in reference 1. The setup of the model on the towing apparatus is shown in figure 4. The model was free to trim about a pivot located at the center of gravity, and was free to move vertically but was restrained laterally and in roll and yaw. During take-offs in rough water and landings in smooth and rough water, the model had 5 feet of fore-and-aft freedom with respect to the towing carriage in order to absorb longitudinal accelerations introduced by the impacts and to permit the model to act as a free body in the longitudinal direction.

A strain-gage-type accelerometer mounted on the towing staff of the model measured the vertical accelerations. Two strain-gage-type accelerometers, mounted 1 foot apart and connected in such a manner that they measured the angular accelerations directly, were located within the model with their centers of gravity in line with the model center of gravity. A mechanical accelerometer, which recorded accelerations on a smoked-glass disk, was mounted in the model just aft of the center of gravity and measured accelerations normal to the keel. In the static condition, all accelerometers read zero. The natural frequencies of the strain-gage accelerometers, the recording galvanometers used with the strain-gage accelerometers, and the mechanical accelerometer, were approximately 180, 40, and 19 cycles per second,

~~CONFIDENTIAL~~

respectively. Both types of accelerometers were damped to approximately 0.7 of their critical values and the recording galvanometers to approximately 0.65 of their critical values. The frequency-response curve of the strain-gage-accelerometer and recording-galvanometer system was flat within ± 5 percent between 0 and 21 cycles per second.

Slide-wire pickups were used to measure the trim, the rise of the center of gravity, and the fore-and-aft position of the model. During landings an electrically actuated trim brake, attached to the towing staff, fixed the trim of the model in the air during the initial approach. The trim brake was automatically released when any of three contacts along the keel touched the water. These contacts, which were located at the sternpost, at the step, and at station 8 on the forebody, also indicated the part of the hull which first entered the water.

The setup used during free-body landings is shown in figure 5. The model was towed from a point above and slightly aft of the center of gravity. The towing apparatus was retracted after launching the model.

Waves were generated by the Langley tank no. 1 wave maker which consists of an oscillating plate hinged at the bottom of the tank and driven by an electric motor. The desired height and length of waves were obtained by a suitable combination of amplitude and frequency of the plate.

PROCEDURES

Aerodynamic

Effective thrust.- The effective thrust of the model, defined as the total drag (power off) plus the resultant horizontal force with power on, was determined at zero trim with the keel just clear of the water surface.

Aerodynamic lift and trim.- The aerodynamic lift and trim with and without power for various flap and elevator deflections were measured with the model free to pivot about the center of gravity and supported so that the sternpost just cleared the water at a trim of 25° .

Air flow.- The air flow over the model at several angles of trim with power on and off was observed by means of tufts attached to the wing, hull, and tail surfaces. Studies were also made with the leading-edge slat removed.

Hydrostatic

Static properties.- The static properties were investigated by means of a movable weight on a transverse beam as shown in figure 6. The angle of heel, trim, and draft for various upsetting moments were recorded.

Jet-exit clearance.- The clearance between the bottom of the jet exit and the water surface was determined in oncoming waves with the model free to pivot about the center of gravity and free to move vertically.

Hydrodynamic

Resistance.- The free-to-trim resistance of the model with the wing removed and of the complete model was determined at constant speeds. A sufficient number of elevator deflections were investigated to determine the minimum resistance for stable trims at each speed. The resistance with the wing removed was determined for loads on the model corresponding to a constant lift coefficient of 1.15.

Trim limits of stability.- The trim limits of stability were determined with and without power at constant speeds by use of the methods described in reference 2.

Center-of-gravity limits of stability.- The center-of-gravity limits of stability for various flap and elevator settings were determined by making accelerated runs to take-off speed with full power and a constant rate of acceleration of 4 feet per second per second. The accelerated runs were made at several center-of-gravity locations in the normal operating range.

Landings with fore-and-aft gear in smooth water and in waves.- The landing stability in smooth water and the landing behavior in waves were investigated by using the fore-and-aft gear. The model was trimmed in the air to the desired landing trim at a speed slightly above flying speed and then the towing carriage was decelerated at a uniform rate; this technique allowed the model to glide onto the water and simulate an actual landing. The landings were made without power and the elevators were set so that the model was approximately in trim at the instant of contact with the water. The rate of deceleration was approximately 4 feet per second per second for contact trims below 14° and approximately $5\frac{1}{2}$ feet per second per second at higher trims to maintain longitudinal freedom. In order to approximate more closely the specified

landing gross weight in waves, the greater part of the rough-water landing investigation was made with the angular accelerometer removed from the model.

Free-body landings in smooth water and in waves.- Free-body landings in smooth water and in waves were made. The model was towed in the air at the desired landing trim and at a speed slightly above flying speed. By suddenly applying brakes to the towing carriage, the model was launched ahead of the carriage as a free body.

Take-off behavior in waves.- The take-off behavior was investigated in waves 8 feet high and of various lengths. The take-offs were made with fixed elevators, full power, and a rate of acceleration of 4 feet per second per second.

Spray characteristics in smooth water.- The smooth-water characteristics with full power were determined in both the upright and heeled (4.25°) conditions. Spray photographs were taken with the model free to trim for a series of constant speeds up to take-off. Simultaneous bow and side photographs were taken to determine spray profiles.

Spray characteristics in rough water.- The spray characteristics in rough water were determined from visual observation and from motion pictures of take-offs and landings.

Drifting characteristics.- The open-water drifting characteristics in the river adjacent to the tank were observed for various headings and motion pictures were made. Additional drift tests were made in Langley tank no. 1 where wind and wave conditions could be more accurately controlled. For the latter tests, a multiengine propeller-driven model attached to the towing carriage was used as the wind source.

RESULTS AND DISCUSSION

All data as presented have been converted to full-size values.

Aerodynamic

The effective thrust as obtained from the model tests is plotted against speed in figure 7. Effective-thrust curves for the airplane, with and without afterburning, furnished by the Bureau of Aeronautics, are shown for comparison.

Aerodynamic-lift coefficient as obtained from tank data is plotted against trim in figure 8 and trim against elevator deflection in figure 9. The effect of power on the lift coefficient was small, but the effect on trim was large. With power, elevator deflections greater than -12.5° immediately trimmed the model up against the stop which was set at 25° .

Photographs of tufts are shown in figure 10 for the power-on condition. The spanwise flow over the wing increased with increase in trim. The wing began to stall near the tip at a trim of approximately 16° and was almost completely stalled at 21° . The flow over the fuselage and tail surfaces was smooth at all trims.

The effect of slats on the leading edge is shown in figure 11. The slotted wing did not begin to stall until approximately 16° trim, whereas the unslotted wing began to stall below 10° trim.

A comparison of the air flow in figure 10 (with power) and the air flow in figure 11 (without power) indicates that the effect of the jets on flow over the wing, hull, and upper surface of the horizontal tail was small. A survey of the flow at zero forward speed indicated that the exhaust from the jet passed below the horizontal tail. The sharp increase in trim with elevator deflection for the power-on condition was probably due to this jet flow between the tail surfaces and the water.

Hydrostatic

Static properties.- Trim, draft, and applied rolling moment are plotted against angle of heel in figure 12. The angle of heel at which the tip float was just submerged is indicated. A small portion of the wing tip was under water when the tip float was just submerged.

An applied upsetting moment of 520,000 pound-feet submerged the tip float at a gross load of 130,000 pounds. The tip float, which has a displacement of 8,200 pounds and a moment arm of 53 feet, had a righting moment of 435,000 pound-feet; thus, the submerged portion of the wing contributed a righting moment of 85,000 pound-feet plus a righting moment equal to the upsetting moment due to the negative metacentric height. The Navy specification for transverse stability of seaplanes (reference 3) requires that the gross righting moment of a submerged wing-tip float must be equal to, or greater than, the value given by the equation

$$c\Delta_t = \Delta_o \left(h_e \sin \phi_1 + \frac{0.10b_w}{\Delta_o/S} + 0.06\sqrt[3]{\Delta_o} \right)$$

which gives a righting moment of 485,000 pound-feet. For the size and position of the tip float used on this design, some submergence of the

wing is required in order to meet this specification, and the outer portion of the wing must, therefore, be watertight.

Jet-exit clearance.- Data on the clearance of the jet exit in waves are presented in table III and the clearance is plotted against length-height ratio of the waves in figure 13. The jet-exit clearance increased with increase in length-height ratio and rapidly approached the clearance in smooth water. The clearance apparently is independent of wave height. The tests indicate sufficient clearance in oncoming waves.

Hydrodynamic

Resistance.- The minimum resistance, load-resistance ratio, and best trim of the hull (with tail surfaces, without the wing) are plotted against speed in figure 14. The load-resistance ratio Δ/R was approximately 4.4 at the hump speed.

The minimum total resistance and best trim of the complete model are plotted against speed in figure 15. The hump resistance occurred at a speed of approximately 72 knots. This resistance was greater than the effective thrust of the assumed power plant at this speed and afterburning would be required to provide the thrust necessary to accelerate past the hump. With afterburning, an excess thrust of 11,000 pounds is available for acceleration at the hump.

Longitudinal acceleration and take-off performance.- The excess thrust was determined by subtracting the resistance shown in figure 15 from the effective thrust, with afterburning, figure 7, and the longitudinal acceleration was computed. This longitudinal acceleration is plotted against speed in figure 16. The acceleration was approximately 3 feet per second per second at the hump and $5\frac{1}{2}$ feet per second per second at high speed. On the basis of these values, a constant acceleration of 4 feet per second per second was selected for use during the accelerated runs to take-off.

Using the longitudinal acceleration of figure 16, the computed take-off time and distance of the full-size airplane are 58 seconds and 5800 feet, respectively.

Trim limits of stability.- The trim limits of stability are presented in figure 17. The effect of power on the trim limits apparently was negligible. In general, the behavior of the model at the trim limits differed appreciably from that of more conventional models. No lower trim limit, below which porpoising occurred, was found. As the trim was increased, however, a trim was reached above which porpoising was encountered.

At constant speeds between 110 and 135 knots, the motion appeared to be similar to the high-angle porpoising of tandem planing surfaces, although the time required to build up to large amplitudes was long. A maximum amplitude of 10° was reached at the end of 15 seconds. In addition, a further increase in elevator deflection greatly reduced the amplitude of porpoising. Apparently, the increase in wetted area of the afterbody with increase in trim provided additional damping to the motion.

At speeds above 135 knots, the motion appeared to be similar to low-angle porpoising and the amplitude of the porpoising was generally divergent. When these large amplitudes were encountered at high speeds, the test run had to be discontinued to avoid possible damage to the model.

Center-of-gravity limits of stability.- Representative trim tracks for various positions of the center of gravity, elevator deflections, and flap deflections are given in figure 18. Reference to figure 17 shows that the trim tracks must intersect the upper trim limit in order to reach take-off speed. As a result, some porpoising was encountered at all center-of-gravity locations and with both flap deflections. This porpoising, however, never exceeded 1.5° at the acceleration of 4 feet per second per second, for take-off speeds below 135 knots and take-off trims above 8° . Divergent porpoising was encountered at higher speeds and lower trims, but it is not considered necessary to reach these conditions during actual take-off.

Center-of-gravity location and elevator deflection had no appreciable effect on the trim tracks at speeds below 90 knots. The effect of flap deflection on the trim tracks was small.

For a given elevator deflection, the practical center-of-gravity limit is usually defined as that position of the center of gravity at which the amplitude of porpoising becomes 2° . Inasmuch as no lower limit was obtained and the upper-limit porpoising never exceeded 1.5° at take-off speeds below 135 knots, practical center-of-gravity limits are nonexistent for the normal operating range from 17 to 32 percent mean aerodynamic chord.

Landing stability in smooth water.- Typical time histories of landings in smooth water at landing trims from 12° to 20° are shown in figure 19 and at 5° and 6.9° in figure 20. From data such as these, the number of skips (number of times the model left the water), maximum and minimum trim and rise, landing speed, deceleration, and flight-path angle were determined and are plotted against landing trim in figure 21.

On landing at trims above the sternpost angle (8.8°), the afterbody contacted the water first, causing the trim to decrease to approximately $7\frac{1}{2}^\circ$ (figs. 19 and 21(b)). The resulting angular velocity and sinking speed caused the model to overshoot the equilibrium position and the trim then increased to a maximum of approximately 14° , but the model did not leave the water (fig. 21(a)) except at the landing trim of 8.9° , when the step just cleared. After approximately three converging cycles, the model reached an equilibrium trim near 12° .

On landing at trims below the sternpost angle, the pointed step contacted the water first and, with the center of gravity aft of this point, the trim increased immediately (figs. 20 and 21(b)) causing the model to leave the water. Inasmuch as the elevators were set for a low landing trim, the trim again decreased and the landing and skipping cycle was repeated. The number of cycles decreased with increase in landing trim. The forward center-of-gravity location resulted in additional skipping but had a negligible effect on the other landing characteristics.

The maximum trim after contact was approximately 14° at all landing trims (fig. 21(b)). The attitude of the model at a trim of 14° is illustrated in figure 22. A large portion of the long afterbody of the planing-tail hull is wetted at this trim and apparently limits the maximum trim after contact to this value.

Although the rise in figure 21(c) is negative for landing trims between 7° and 9° , the model still left the water as shown in figure 21(a) since the rise is that of the center of gravity and not of the step. The actual distance between the center of gravity and the water surface is appreciably less at high trims than the distance between the center of gravity and the step.

An increase in deceleration of 1 foot per second per second at a landing trim of 14° had a negligible effect on the smooth-water landing characteristics. The flight-path angle during the landing approach increased with increase in landing trim to a maximum of about 1.9° at a landing trim of 15° . Above 15° the flight-path angle decreased.

With the center of gravity at 20 percent mean aerodynamic chord and with 50° flaps, the maximum trim in the air obtainable with full-up elevators was 6.9° . This low landing trim necessarily results in high landing speeds, increased porpoising, and skipping, making landings at forward positions of the center of gravity difficult. High trims can be obtained with more aft positions of the center of gravity, however, and a practicable minimum landing trim might be taken as 12° with a landing speed of 110 knots. At landing trims above 12° , some oscillation

in trim was encountered, but since the oscillations damped out rapidly, the landing behavior appears to be acceptable in this range.

Free-body landings in smooth water.- Typical paths of the model during free-body landings in smooth water are shown in figure 23. The basic model had a violent tendency to turn to the left at relatively high speeds. A careful check of the model did not reveal any asymmetry or other defect in the planing bottom which could cause this directional instability.

As a corrective measure, a small skeg was added to the keel at the sternpost as shown in figure 24. Although the model continued to turn to the left, the skeg tended to straighten the path of the model and the violent turn was eliminated. Additional fin area of 11 percent was next added to the vertical-tail surface (fig. 24). With the additional fin area, but with the skeg removed, the violent turn was likewise eliminated. The model could be made to turn either right or left by deflection of the added fin, but a straight path down the tank could not be obtained. The landing path of the model with both the skeg and the additional fin area (fig. 23) showed no directional instability.

Landing behavior in waves.- Pertinent data for the initial impact and the impact which resulted in the maximum acceleration during landings at three landing trims in waves 340 feet long are given in table IV. Similar data at a trim of 12° in waves of various lengths are given in table V.

The effects of landing trim on the maximum vertical and angular accelerations, and the maximum and minimum trim and rise in 8-foot waves are shown in figure 25. Inasmuch as these effects were negligible, the effects of wave length were investigated at only one landing trim. These effects are shown in figure 26. The position of landing on a wave for the initial impact as well as subsequent impacts during the landing run was not under the control of the operator, and this lack of control accounts for the scatter of test data. The envelopes of the data indicate the maximum values obtained. A maximum vertical acceleration of approximately 9g was obtained in waves 8 feet high and 200 feet long. This was the shortest regular wave which could be obtained for this wave height. The maximum acceleration was reduced with increase in wave length, approximately 5.5g being obtained at a wave length of 580 feet.

The maximum and minimum trim did not vary greatly with wave length. A maximum trim of about 20° was obtained. The maximum rise varied greatly with wave length. A maximum rise of approximately 16 feet was obtained at wave lengths near 300 feet. This maximum was reduced to approximately 6 feet at a wave length of 580 feet.

The maximum accelerations normal to the keel recorded by the mechanical accelerometer and the envelope of maximum vertical accelerations obtained with the strain-gage accelerometer during the same landings are shown in figure 27. Because of the lower frequency response of the mechanical type, it was preset to 3g and only accelerations in excess of this value were indicated. The resulting maximums were slightly lower than those obtained with the strain-gage type, presumably because of the lower frequency response.

Free-body landings in waves.- During rough-water landings with the fore-and-aft gear, the model tended to yaw, but because of the lateral restraint, the yawing appeared as a twisting motion. This motion was so violent during some landings that the run was discontinued to prevent damage. The skeg and additional fin area were therefore added, as shown in figure 24, before the model was launched as a free body in rough water. During most of the free-body landings in waves, the model followed a fairly straight course down the tank. The only evidence of directional instability was a slight tendency to turn when the skeg came clear of the water as the model trimmed down. The wing-tip floats provided the necessary righting moment if one wing tended to drop as the model bounced off the waves. The entrance of a tip float in the water before the hull did not appear to cause a tendency to turn.

The maximum normal accelerations obtained during the free-body landings in waves are plotted against wave length in figure 28. The maximum normal accelerations were approximately the same as those obtained when the model was attached to the fore-and-aft gear.

Take-off behavior in waves.- The characteristics obtained during accelerated take-offs in 8-foot waves are plotted against wave length in figure 29. The envelopes for landings are shown for comparison. These data indicate that the maximum vertical accelerations and the motions in trim and rise were approximately the same for take-off as for landing.

Spray characteristics in smooth water.- The forebody spray during take-off with power is shown in figure 30. The jet intakes were clear of spray throughout the speed range to take-off. Spray struck the flaps over the speed range between 27 and 44 knots as shown in figure 31. This spray was heavy over the speed range between 32 and 39 knots.

The spray during landings without power is shown in figure 32. Blister spray from the forebody struck the tail surfaces over the range of speed from approximately 50 knots to 100 knots. This blister spray was heavy and might necessitate raising the horizontal-tail surfaces which would be clear if raised approximately 5 feet.

The envelopes of blister spray for the upright and heeled conditions are shown in figure 33. The envelopes for the profile view are lines drawn tangent to the spray blisters for a series of constant-speed runs. The envelopes for the plan and front views are lines drawn through the peaks of the spray blisters. These spray envelopes also indicate sufficient clearance of the jet air intakes for take-off.

Spray characteristics in rough water.- At low speeds, blister spray in 8-foot waves struck the flaps over a short speed range. The forebody spray striking the horizontal-tail surfaces at high speeds was heavy and the elevators were damaged during several landings. Typical spray on the tail and damage to the port elevator are shown in figure 34. These photographs are enlargements of 16-millimeter motion pictures.

Bow spray entered the jet air-intake ducts during landings in waves 8 feet high and 204 feet long as shown in figures 35 and 36. This bow spray was encountered at low speeds when the model was following the wave profile. Inasmuch as the landings were made without power, only a small amount of spray actually entered the ducts, although the photographs indicate that the spray over the bow was heavy. During accelerated runs to take-off with power, the model trimmed up and no spray entered the air intakes throughout the range of wave length investigated.

Drifting characteristics.- The model at a gross load corresponding to 62,000 pounds (empty weight) drifted slowly when set adrift in $1\frac{1}{2}$ -foot waves with a wind velocity of 20 knots and generally drifted at the same heading with respect to the wind as when released. When released with a downwind heading, however, a crosswind heading was assumed and drifting continued with this heading.

When set adrift in 10-foot waves with a wind velocity of 60 knots, the model overturned several times during the tests. This overturning occurred when a crosswind heading was assumed with the hull on the crest of a wave and the downwind tip float in a trough.

The open-water investigation of the drifting characteristics indicated that the basic design had insufficient weather-cock stability and a sea anchor would be necessary to keep the bow into the wind in order to prevent a heading which could result in overturning.

The drifting characteristics in the tank are presented in figure 37. When released with upwind, downwind, or crosswind headings, the model slowly turned to, and drifted at, a heading of approximately 40° to the wind direction. Approximately 40 seconds were required to assume this heading. These tests substantiated the conclusion reached from the open-water tests, that the design had poor drifting characteristics.

CONCLUSIONS

The results of the investigation of the hydrodynamic characteristics of a $\frac{1}{17}$ -size jet-powered dynamic model of the DR 56 flying boat led to the following conclusions:

1. A small portion of the wing tip was under water when the tip float was just submerged; the combination of submerged wing and tip float provided sufficient righting moment to meet Navy specifications.
2. At hump speed, the load-resistance ratio of the hull without the wing was approximately 4.4 and the total resistance was greater than the effective thrust of the assumed power plant without afterburning. The computed take-off time and distance with afterburning were 58 seconds and 5800 feet (full size), respectively.
3. Take-offs were longitudinally stable at all center-of-gravity locations in the normal operating range.
4. Oscillations in trim were obtained at all landing trims in smooth water, but the oscillations damped out rapidly, and the landing behavior appeared to be acceptable at trims above 12° .
5. Poor directional stability was encountered at high speeds during landings, but was improved by use of additional vertical-fin area and a small skeg at the sternpost.
6. Variations in landing trim from 11° to 20° had a negligible effect on the maximum trim, rise, and vertical and angular accelerations during landings in 8-foot waves (full size). A maximum vertical acceleration of approximately 9g was obtained.
7. The jet air intakes were clear of spray except at low speeds in short waves. The flaps were heavily wetted over a short speed range. The tail surfaces were heavily wetted over a wide speed range and might have to be raised to avoid damage in rough water.

8. The drifting characteristics indicated insufficient weathercock stability.

Langley Aeronautical Laboratory
National Advisory Committee for Aeronautics
Langley Field, Va.

REFERENCES

1. Truscott, Starr: The Enlarged N.A.C.A. Tank, and Some of Its Work. NACA TM 918, 1939.
2. Olson, Roland E., and Land, Norman S.: Methods Used in the NACA Tank for the Investigation of the Longitudinal-Stability Characteristics of Models of Flying Boats. NACA Rep. 753, 1943.
3. Anon.: Specification for Transverse Stability of Seaplanes - Displacement and Location of Auxiliary Floats. NAVAER SR-59C (superseding SR-59B), Bur. Aero., Feb. 20, 1942.

~~CONFIDENTIAL~~

TABLE I

OFFSETS FOR LANGLEY TANK MODEL 248

[All dimensions are in inches]

Station	Distance to F.P.	Height above base line											Half-breadth								
		Keel	Chine	Cove	Hull at center line	Buttock.							Chine	Cove	Water line						
						0.36	0.72	1.08	1.44	1.80	2.16	2.52			2.59	3.98	4.73	5.75	6.78	7.73	8.70
F.P.	0	4.75			4.75																
1/4	0.35	3.98			5.16	4.23 5.04											0.55				
1/2	.71	3.43			5.40	3.83 5.30	4.15 5.01										0.46	.82			
1	1.41	2.60			5.77	3.19 5.69	3.53 5.47	3.78 4.95									1.23	1.17			
1 1/2	2.12	1.98	3.39		6.10	2.52 6.03	2.98 5.83	3.28 5.45	3.39 4.55				1.51		0.40	1.52	1.40	0.81			
2	2.83	1.53	3.07		6.42	1.98 6.34	2.46 6.17	2.87 5.83	3.06 5.16				1.74		.80	1.68	1.57	1.13			
4	5.65	.49	2.31		7.42	.83 7.39	1.21 7.24	1.59 6.96	1.91 6.50	2.19 5.85	2.32 4.48		2.36		2.34	2.22	2.10	1.84	1.23		
6	8.48	.11	1.92		8.20	.39 8.17	.68 8.04	.97 7.83	1.26 7.48	1.54 7.01	1.81 6.30	1.92 4.89	2.77		2.74	2.63	2.53	2.35	1.91	1.18	
8	11.31	0	1.68		8.75	.23 8.72	.47 8.63	.71 8.42	.94 8.11	1.16 7.74	1.41 7.04	1.60 6.14	3.02		2.98	2.89	2.80	2.63	2.26	1.77	0.45
10	14.13	0	1.53		9.18	.20 9.15	.41 9.03	.63 8.84	.83 8.53	1.02 8.14	1.23 7.47	1.42 6.66	3.17		3.11	3.01	2.92	2.76	2.43	2.04	1.22
12	16.96	0	1.42		9.43	.19 9.41	.40 9.29	.63 9.08	.83 8.75	1.02 8.31	1.22 7.68	1.35 6.82	3.18		3.13	3.04	2.97	2.80	2.50	2.11	1.48
14	19.79	0	1.33	4.01	9.53	.19 9.50	.40 9.42	.63 9.18	.83 8.82	1.02 8.34	1.19 7.68	1.31 6.82	3.05	3.05	3.04	3.01	2.97	2.80	2.52	2.11	1.55
16	22.61	0	1.21	3.65	9.53	.19 9.50	.40 9.42	.63 9.18	.83 8.82	1.01 8.34	1.16 7.68	1.21 6.82	2.76	2.76	2.77	2.91	2.97	2.80	2.52	2.11	1.55
18	25.44	0	1.02	3.32	9.53	.19 9.50	.40 9.42	.63 9.18	.83 8.82	.96 8.34	1.03 7.68	3.56 6.82	2.24	2.24	2.24	2.79	2.97	2.80	2.52	2.11	1.55
20	28.27	0	.68	3.13	9.53	.19 9.50	.40 9.42	.58 9.18	3.20 8.82	3.34 8.34	3.54 7.68	3.83 6.82	1.42	1.42	1.42	2.65	2.92	2.80	2.52	2.11	1.55
22	31.09	0	.16	3.15	9.53	3.18 9.50	3.23 9.42	3.31 9.18	3.42 8.82	3.57 8.34	3.74 7.68	4.11 6.82	.34	.34	.35	2.41	2.85	2.80	2.52	2.11	1.55
Step	31.80	0 3.18	0	3.18	9.53	3.22 9.50	3.28 9.42	3.36 9.18	3.46 8.82	3.62 8.34	3.84 7.68	4.20 6.82	.06	.06	.06	2.40	2.81	2.80	2.52	2.11	1.55
26	36.75	3.53			9.53	3.58 9.50	3.67 9.42	3.73 9.18	3.90 8.82	4.07 8.34	4.34 7.68	4.80 6.82				1.64	2.52	2.70	2.52	2.11	1.55
30	42.40	3.96	5.03		9.53	4.07 9.50	4.13 9.42	4.18 9.18	4.39 8.82	4.59 8.34	4.83 7.63		2.33			.15	2.01	2.49	2.47	2.11	1.55
34	48.06	4.37	5.09		9.53	4.46 9.50	4.56 9.42	4.70 9.18	4.85 8.82	5.08 8.34	5.75 7.52		2.07			1.24	2.19	2.28	2.08	1.55	
38	53.71	4.76	5.20		9.53	4.85 9.50	4.99 9.42	5.14 9.18	5.28 8.82	5.60 8.18			1.78				1.84	1.99	1.93	1.55	
42	59.36	5.18	5.46		9.53	5.29 9.50	5.42 9.42	5.55 9.14	5.70 8.70				1.44				1.43	1.62	1.66	1.45	
46	65.02	5.58	5.81		9.53	5.73 9.46	5.88 9.26	6.63 8.77					.86				.44	1.10	1.27	1.13	
A.P.	68.76	5.86	6.06		9.53	6.37 9.40	7.53 8.75						.24					.50	.77	.74	

NACA

TABLE II

PERTINENT CHARACTERISTICS AND DIMENSIONS OF
BUREAU OF AERONAUTICS DESIGN DR 56 FLYING BOAT
AND LANGLEY TANK MODEL 248

	<u>Model</u>	<u>Full Size</u>
General:		
Design gross load, lb	26.46	130,000
Gross-load coefficient, C_{Δ_0}	2.79	2.79
Wing area, sq ft	6.44	1860
Thrust:		
Static, lb	6.1	30,000
With afterburning at 600 mph at 35,000 ft, lb		55,500
Over-all length, ft	6.62	112.5
Hull:		
Maximum beam, ft	0.53	9.0
Length:		
Forebody, bow to step, ft	2.65	45.0
Forebody length-beam ratio	5.0	5.0
Afterbody, step to sternpost, ft	3.18	54.0
Afterbody length-beam ratio	6.0	6.0
Step:		
Type	Pointed	Pointed
Depth at keel, in.	3.18	54.0
Depth at keel, percent beam	50	50
Angle of forebody keel to base line, deg	0	0
Angle of afterbody keel to base line, deg	4.1	4.1
Sternpost angle, deg	8.8	8.8
Wing (NACA 64(212)-214 normal to 25-percent-chord line):		
Span (center line of tip floats), ft	6.24	106
Mean aerodynamic chord:		
Length, projected, ft	1.09	18.5
Leading edge aft of bow, ft	2.68	45.6
Leading edge aft of step, ft	0.03	0.5
Leading edge above base line, ft	0.96	16.3
Aspect ratio	6	6



~~CONFIDENTIAL~~

TABLE II

PERTINENT CHARACTERISTICS AND DIMENSIONS OF
BUREAU OF AERONAUTICS DESIGN DR 56 FLYING BOAT
AND LANGLEY TANK MODEL 248 - Concluded

	<u>Model</u>	<u>Full Size</u>
Taper ratio	2.5	2.5
Sweepback (25-percent-chord line), deg . . .	35	35
Angle of incidence, deg	3	3
Wing-tip float:		
Maximum beam, ft	0.19	3.2
Length, ft	1.47	25.0
Length-beam ratio	7.8	7.8
Displacement, lb	1.67	8200
Horizontal-tail surfaces:		
Area, sq ft	1.28	370
Span, ft	2.41	41
Length from 20 percent M.A.C. of wing to hinge of elevators at hull center line, ft	2.95	50.2
Height above base line at hull center line, ft	1.28	21.8



~~CONFIDENTIAL~~

TABLE III

DATA ON CLEARANCE OF JET EXIT FOR
BUREAU OF AERONAUTICS DESIGN DR 56 FLYING BOAT

Wave height (ft)	Wave length (ft)	^a Minimum clearance of jet exit (ft)	Maximum trim (deg)	Minimum trim (deg)	^b Maximum draft (ft)	Minimum draft (ft)	At minimum clearance	
							Trim (deg)	Draft (ft)
0		3.9	6.5		8.0			
4	85	2.6	12.4	3.8	8.3	6.6	4.3	7.5
	135	3.4	10.4	4.8	8.7	6.5	5.2	7.0
	170	3.6	11.4	4.0	8.5	6.3	8.5	6.6
	205	3.7	9.2	5.4	9.0	6.3	8.6	7.7
	270	3.6	10.7	5.8	8.7	6.8	9.9	7.5
8	100	1.7	14.8	2.6	9.4	5.3	6.5	8.3
	135	2.4	13.9	2.5	9.0	5.6	4.4	8.5
	205	2.9	14.5	3.0	11.2	4.6	13.5	9.4
	270	2.9	12.4	4.2	9.7	4.8	10.7	8.0

^aMinimum clearance of jet exit is the distance between the bottom of the jet exit and the water.

^bZero draft was measured with the step just touching the water at zero trim. Draft in waves is referred to the undisturbed water surface.



TABLE IV

DATA OBTAINED DURING LANDINGS IN WAVES 8 FEET HIGH AND 340 FEET LONG
BUREAU OF AERONAUTICS DESIGN DR 56 FLYING BOAT

Landing	τ_L (deg)	Initial impact						Maximum acceleration						
		τ (deg)	V_v (fpm)	V (knots)	γ (deg)	n_v (g)	a ($\frac{\text{radians}}{\text{sec}^2}$)	Impact	τ (deg)	V_v (fpm)	V (knots)	γ (deg)	n_v (g)	a ($\frac{\text{radians}}{\text{sec}^2}$)
1	11.0	2.0	737	101.3	4.12	5.1	4.7	2	6.6	1163	90.3	7.25	8.2	10.4
2	11.0	3.6	542	102.5	2.98	4.2	8.1	2	7.6	918	92.0	5.62	7.0	7.8
3	11.0	11.0	473	102.2	2.60	4.8	3.5	4	6.4	631	81.7	4.36	5.7	8.8
	11.0	5.4	594	103.0	3.27	4.8	8.2	4	4.6	873	73.7	6.66	7.8	10.6
5	11.0	4.8	485	97.8	2.80	4.6	6.6	4	3.4	891	75.6	6.63	8.0	11.6
								6	4.3	1064	61.7	9.65	7.3	7.1
6	11.2	11.0	572	100.8	3.20	5.2	4.6	4	4.7	829	68.6	6.80	7.1	10.0
	11.3	11.3	443	100.5	2.50	4.0	4.8	6	4.6	960	65.4	8.23	7.3	10.7
8	11.4	10.4	609	97.4	3.53	7.0	8.5	4	5.0	811	72.4	6.30	7.7	10.0
								1	10.4	609	97.4	3.53	7.0	8.5
9	15.0	14.8	547	95.2	3.23	2.7	3.6	4	5.0	896	68.3	7.37	6.4	9.6
	15.2	12.1	552	97.6	3.18	4.0	3.4	3	5.9	683	79.8	4.82	7.0	10.6
11	15.2	2.7	826	95.9	4.87	3.9	4.6	3	4.0	722	80.5	5.06	6.5	10.1
	15.2	3.4	530	95.2	3.15	2.1	4.1	3	5.6	905	76.4	6.67	6.5	8.6
12								3	5.9	589	83.0	4.00	3.8	5.9
								6	6.6	589	87.4	3.80	3.6	6.1
13	15.2	14.1	349	100.8	2.35	2.0	2.9	6	4.3	881	70.0	7.01	7.2	10.0
14	15.3	12.5	443	98.1	2.55	2.9	3.1	3	3.6	851	78.1	6.13	7.7	9.2
15	15.4	7.8	482	95.2	2.87	4.3	4.9	4	4.8	774	78.1	5.58	7.1	10.5
16	20.0	8.0	626	94.4	3.73	4.5	6.9	6	6.4	873	69.0	7.10	6.8	10.4
17	20.3	7.2	512	90.8	3.18	4.0	5.8	3	3.4	834	74.4	6.30	7.5	9.9
18	20.4	1.7	816	96.9	4.75	4.8	7.1	5	5.9	871	68.8	7.12	6.7	9.4
19	20.4	12.1	391	94.7	2.33	2.8	2.6	5	5.1	881	70.3	7.05	7.2	11.4
20	20.4	5.0	621	92.2	3.60	2.8	3.2	3	5.1	700	78.1	5.05	6.5	8.4
								6	6.4	631	84.9	4.19	5.9	9.4
21	20.5	6.0	876	92.2	5.35	6.9	11.1	1	6.0	876	92.2	5.35	6.9	11.1
22	20.5	1.8	846	94.2	5.07	6.8	9.3	5	4.6	928	67.1	7.75	6.9	10.6
23	20.5	8.0	683	94.4	4.08	6.2	7.4	4	5.9	1002	68.3	8.23	7.3	10.0
24	20.6	14.1	507	95.4	3.00	2.4	3.6	4	4.9	851	75.6	6.33	7.2	10.3
								6	5.4	990	64.4	8.62	5.9	11.5
25	20.6	3.7	386	94.7	2.32	5.5	9.6	6	5.3	841	73.2	6.47	7.2	11.2

^aImpact for maximum angular acceleration

NACA

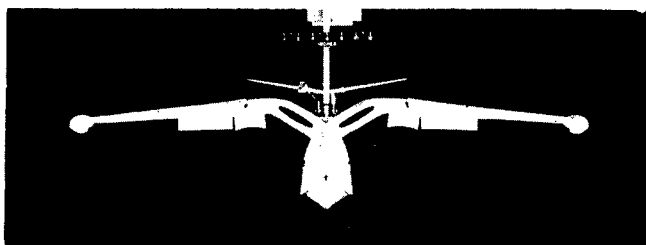
TABLE V

DATA OBTAINED DURING LANDINGS IN 8-FOOT WAVES
BUREAU OF AERONAUTICS DESIGN DR 56 FLYING BOAT

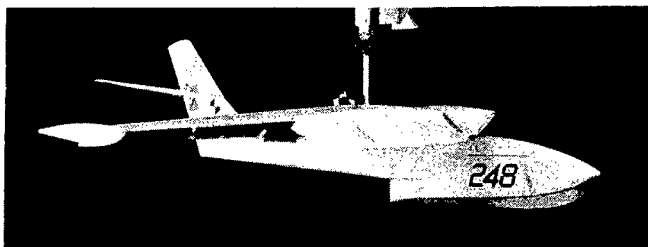
Landing	Wave length (ft)	τ_L (deg)	Initial impact					Maximum acceleration					
			τ (deg)	V_V (fpm)	V (knots)	γ (deg)	n_V (g)	Impact	τ (deg)	V_V (fpm)	V (knots)	γ (deg)	n_V (g)
26	194	11.1	11.1	321	89.5	2.20	4.2	4	6.0	623	76.1	4.62	5.2
27	197	11.1	5.4	598	92.5	3.65	5.5	3	4.1	724	78.1	5.23	6.4
28	204	11.0	6.0	---	87.6	---	7.3	3	6.4	---	69.5	---	9.3
29	204	11.1	4.3	561	83.9	3.78	4.5	3	9.0	502	76.9	3.68	8.6
30	209	11.2	6.4	230	92.7	1.40	5.9	4	2.2	902	68.3	7.42	7.6
31	219	11.2	2.5	554	85.4	3.74	5.7	2	5.2	774	75.2	5.80	8.9
32	226	11.0	3.1	529	85.4	3.50	2.8	3	3.0	850	73.7	6.50	7.6
33	253	12.4	2.7	591	93.0	3.60	4.8	6	7.6	695	63.4	6.20	7.1
34	258	12.5	7.2	509	93.2	3.08	6.9	3	2.5	1115	76.6	8.20	8.3
35	258	11.0	3.5	452	94.2	2.72	3.9	5	7.0	734	61.5	6.72	6.6
36	260	11.0	4.9	569	93.2	3.45	6.1	1	4.9	569	93.2	3.45	6.1
37	265	11.3	11.3	334	93.0	2.03	4.3	5	7.8	858	63.9	7.55	5.8
38	267	12.5	4.2	497	95.2	2.93	6.1	2	10.2	771	85.9	5.10	7.0
39	269	12.5	3.2	529	91.3	3.25	5.6	3	5.5	719	69.5	5.80	5.8
40	269	11.3	2.8	576	94.4	3.45	6.0	4	10.0	850	63.9	7.50	6.7
41	277	11.0	3.3	485	95.2	2.88	4.0	7	7.4	712	63.0	6.37	6.6
42	279	11.3	3.5	633	89.3	4.00	5.8	6	5.0	895	62.2	8.10	6.8
43	280	11.0	7.4	361	94.7	2.15	2.7	6	11.4	564	67.8	4.70	6.7
44	284	11.2	1.8	536	97.1	3.10	7.6	1	1.8	536	97.1	3.10	7.6
45	287	11.0	7.8	485	94.9	2.88	5.2	2	6.7	690	77.6	5.02	5.9
46	287	11.1	5.4	544	86.6	3.55	5.6	4	4.8	922	59.3	8.70	7.7
47	291	11.1	1.2	598	90.8	3.72	3.1	4	5.0	806	59.0	7.70	8.0
48	291	11.4	11.4	457	87.8	2.95	4.5	5	9.3	709	68.1	7.30	5.8
49	291	11.0	1.4	551	90.3	3.45	6.7	3	11.0	789	80.3	5.55	6.7
50	308	11.3	1.6	680	93.0	4.13	3.9	5	4.5	959	62.7	8.60	6.5
51	314	11.0	.8	519	93.0	3.12	4.8	2	7.5	895	83.0	6.10	7.6
52	320	12.5	8.1	386	99.6	2.20	3.4	7	6.6	794	71.5	6.20	6.3
53	325	11.2	11.2	329	96.9	1.90	3.5	5	5.0	1127	62.5	10.10	6.0
54	337	12.5	2.7	578	99.3	3.30	3.2	2	7.5	865	92.7	5.20	7.2
55	340	12.2	4.4	480	97.4	2.78	3.7	7	6.4	853	67.8	7.10	6.1
56	340	12.2	2.3	578	98.1	3.33	5.5	10	5.1	981	62.7	8.80	6.2
57	340	11.0	1.7	566	92.7	3.45	3.2	4	4.0	796	63.4	7.05	6.9
58	379	11.2	11.2	334	96.4	2.00	2.9	5	6.1	870	70.8	6.90	7.3
59	382	11.1	11.1	341	91.0	2.12	2.7	3	1.7	984	66.9	8.30	7.7
60	384	11.2	2.4	677	94.2	4.00	4.6	4	3.8	999	66.6	8.40	7.4
61	386	11.6	1.2	754	90.0	4.72	4.7	3	2.8	939	72.0	7.30	5.0
62	388	11.2	11.2	309	95.2	1.90	2.9	3	2.9	974	70.8	7.70	7.2
63	394	11.1	11.1	373	92.2	2.30	2.1	5	3.2	920	67.8	7.60	7.2
64	394	11.1	11.1	274	93.9	1.60	3.3	3	2.6	974	69.3	7.90	7.9
65	396	11.1	5.0	620	90.3	3.80	6.1	3	2.8	902	70.8	7.20	6.3
66	427	12.2	12.2	391	89.5	2.47	3.7	4	3.9	905	61.5	8.30	7.7
67	427	11.2	11.2	410	93.2	2.50	3.2	4	2.7	952	71.5	7.50	6.6
68	440	11.9	3.3	754	90.0	4.73	4.2	4	2.9	875	67.3	7.30	7.0
69	442	12.3	3.4	591	95.9	3.65	3.6	4	4.0	850	77.6	6.20	6.2
70	442	12.3	7.4	405	99.6	2.30	4.7	6	2.0	979	74.4	7.40	6.0
71	442	12.2	3.6	596	97.6	3.45	3.8	5	4.9	840	79.5	6.00	6.2
72	442	12.2	6.0	522	96.9	3.06	4.2	4	4.1	878	78.8	6.30	7.0
73	452	11.3	11.3	480	91.7	3.00	3.6	3	2.8	952	70.8	7.60	5.8
74	529	12.2	11.6	391	89.3	2.47	2.1	2	2.6	796	82.0	5.48	4.3
75	544	12.2	10.4	445	92.7	2.70	2.8	2	3.4	828	87.8	5.32	4.6
76	544	12.2	7.0	497	93.0	3.03	2.6	1	7.0	497	93.0	3.03	2.6
77	544	12.2	8.8	440	94.2	2.63	2.1	2	5.8	709	89.5	4.43	3.8
78	544	12.2	12.1	163	100.0	.92	1.1	4	3.7	808	85.4	5.37	5.4
79	549	11.3	6.8	719	92.7	4.38	2.2	2	6.8	719	92.7	4.40	2.2
80	551	12.4	10.6	494	92.2	3.03	3.0	2	3.6	942	83.0	6.38	5.4
81	556	12.2	6.1	695	87.8	4.47	3.0	2	4.0	865	78.8	6.18	3.8
82	576	11.3	11.2	420	94.9	2.50	2.4	2	2.5	808	87.6	5.20	5.7
83	581	12.5	10.3	292	92.2	1.78	1.0	2	5.1	658	80.0	4.63	1.5

NACA

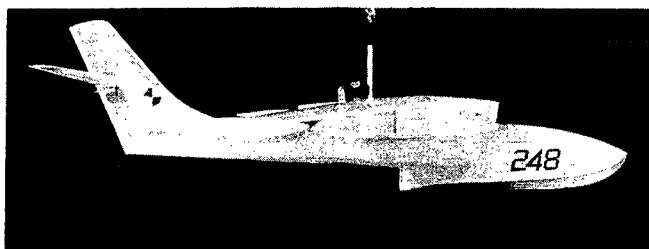
CONFIDENTIAL



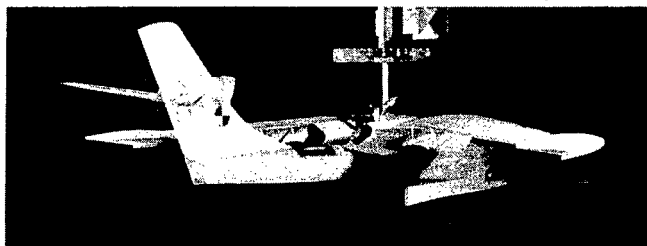
Front view



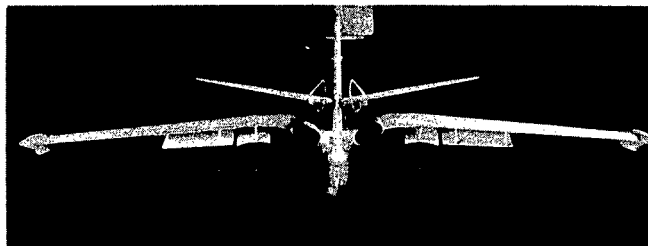
Three-quarter front view



Side view



Three-quarter rear view



Rear view

Figure 1.- Langley tank model 248.

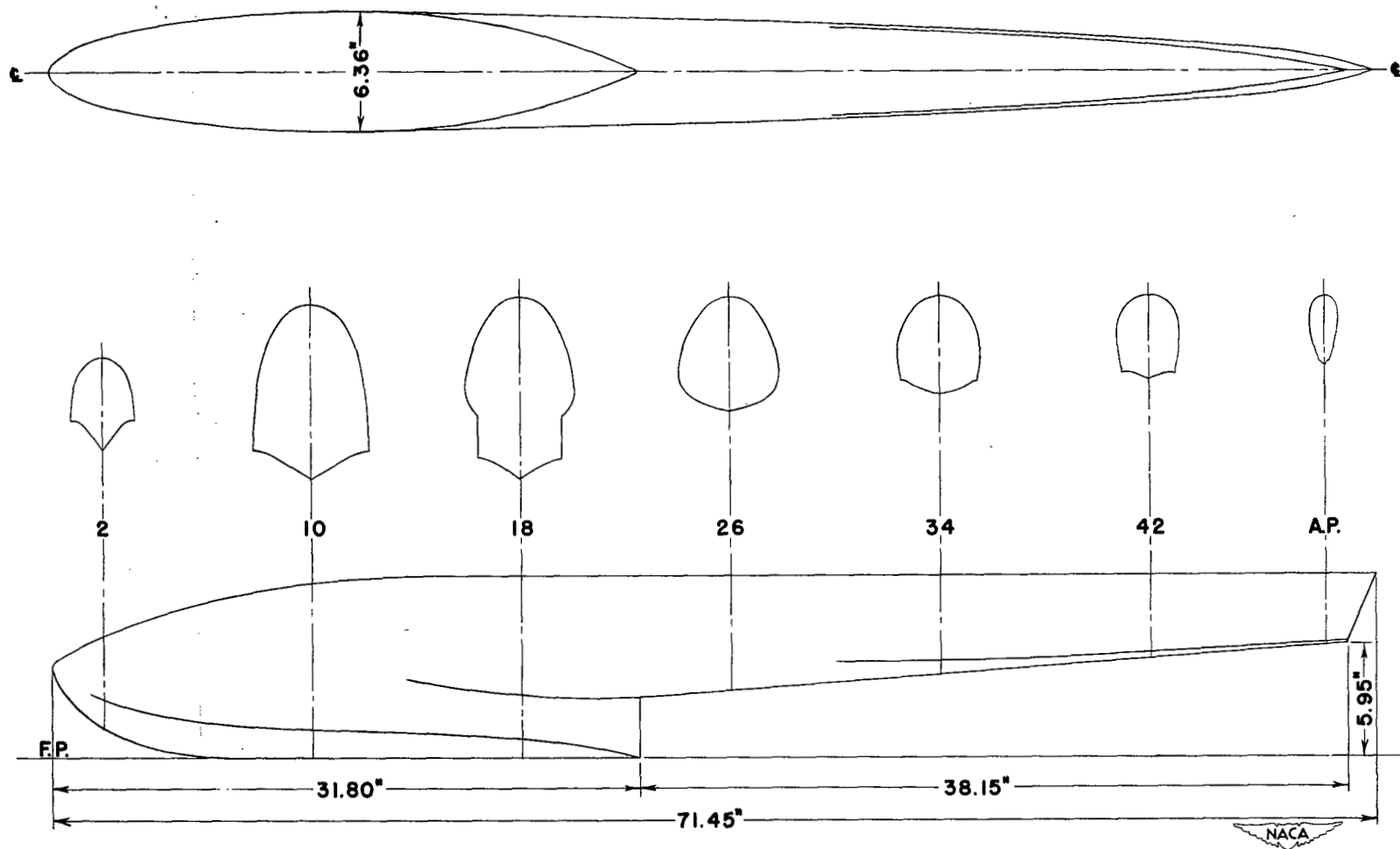


Figure 2.- Hull lines of Langley tank model 248.

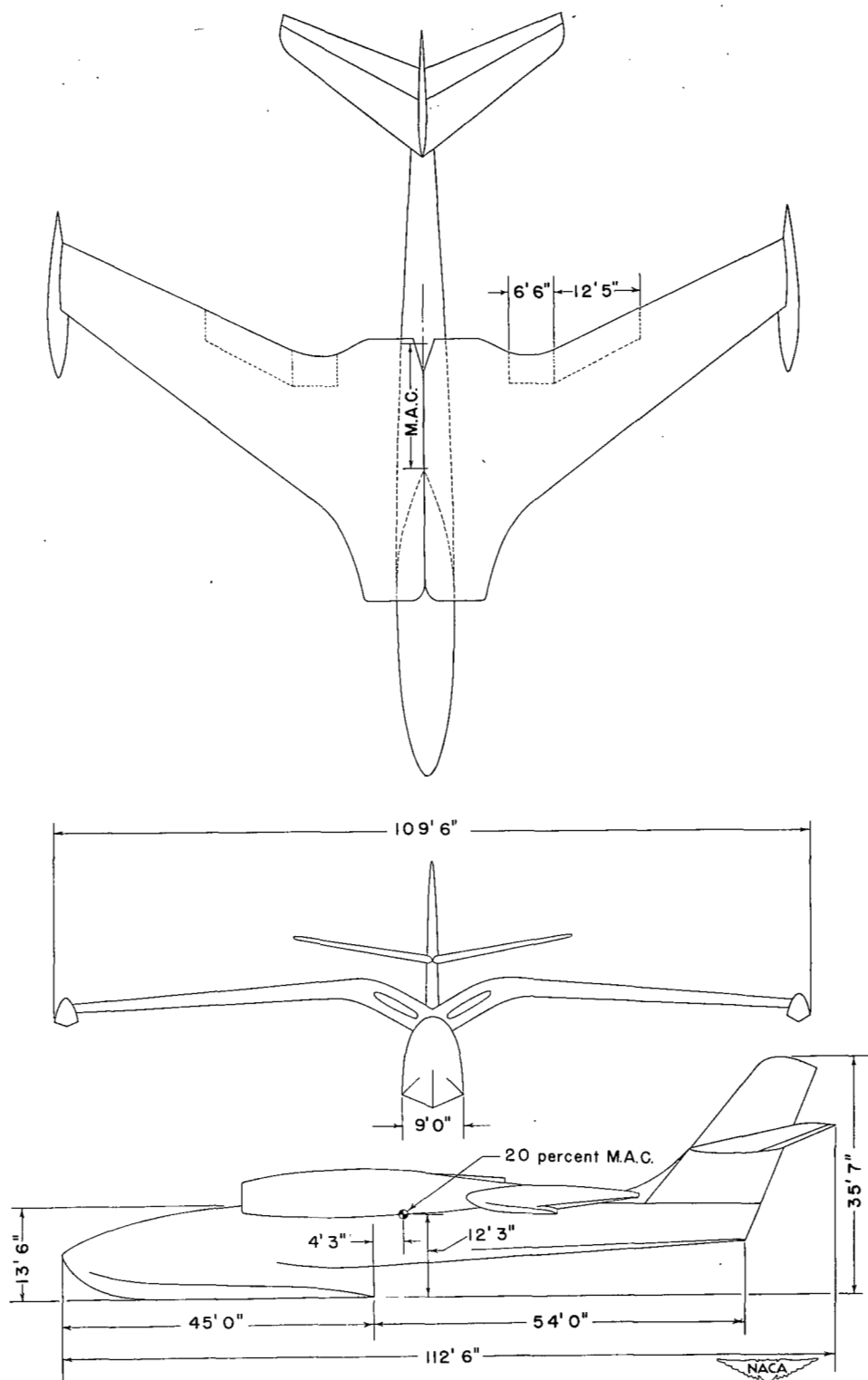


Figure 3.- General arrangement.

~~CONFIDENTIAL~~

CONFIDENTIAL

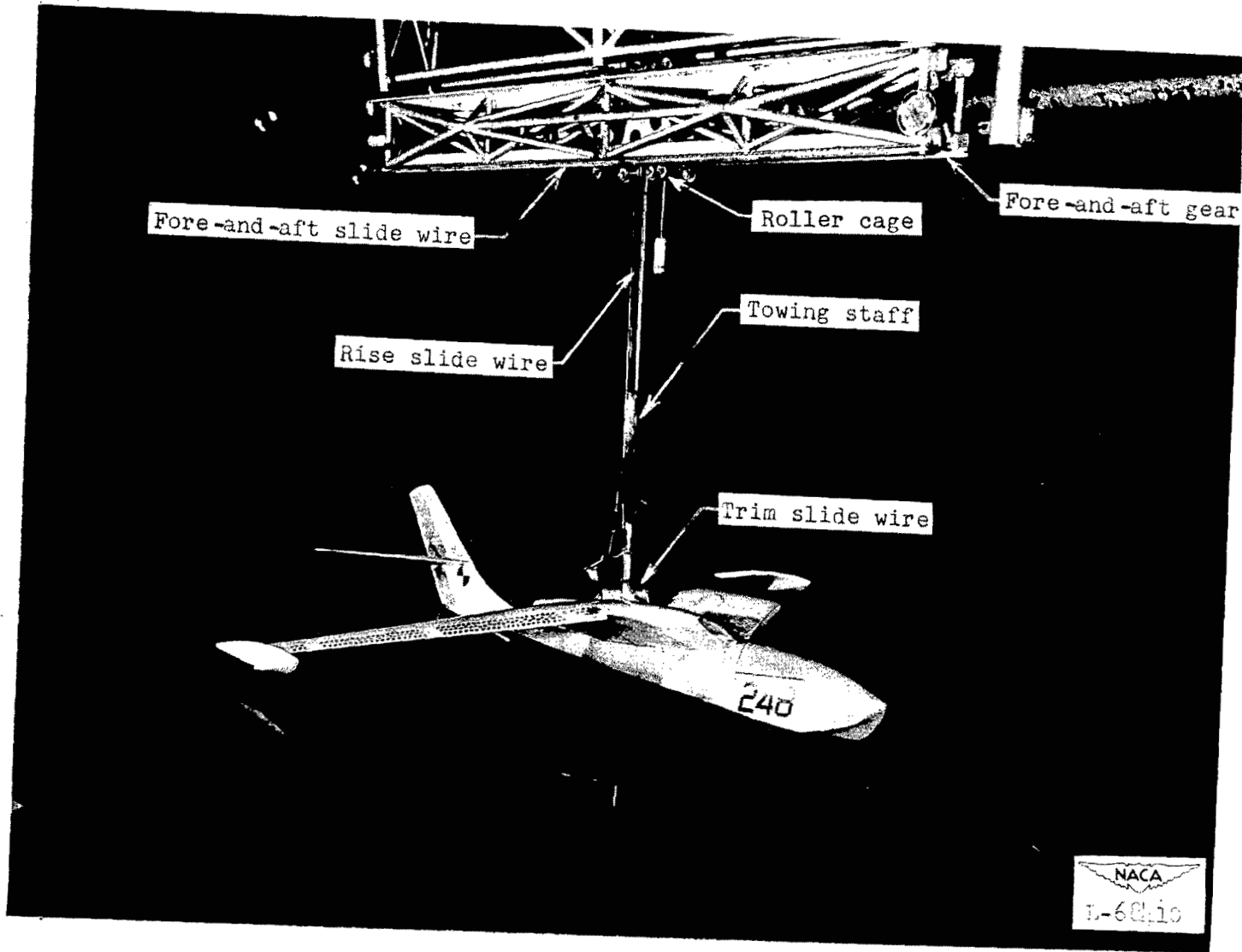


Figure 4.- Setup of model on towing apparatus.

CONFIDENTIAL

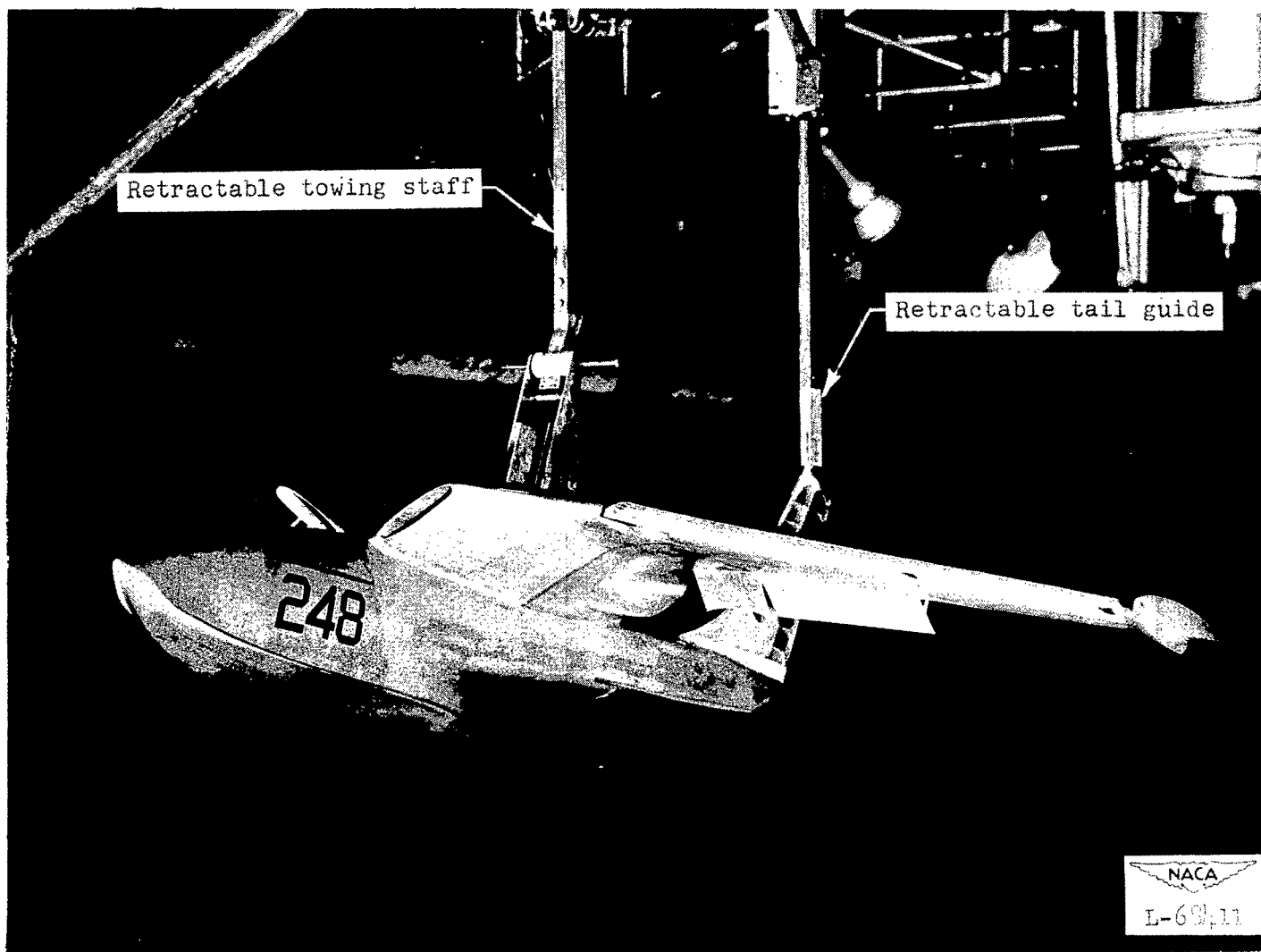


Figure 5.- Setup of model and apparatus for launching model as free body.

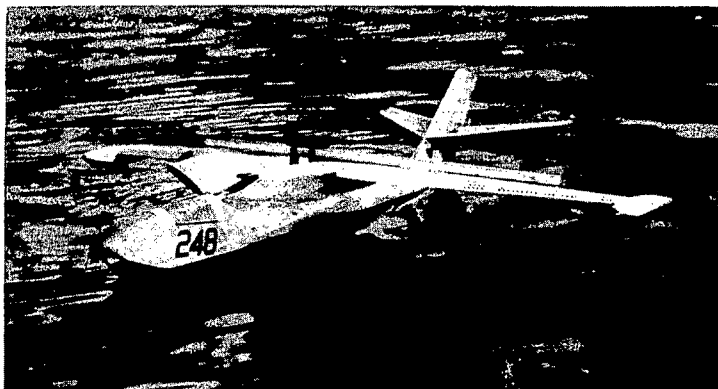
Angle of heel, 2.6° Angle of heel, 6.9° Angle of heel, 13.6°

Figure 6.- Photographs of model at three angles of heel. Δ_0 , 130,000 pounds; center-of-gravity location, 32 percent mean aerodynamic chord.

NACA
L-68412

CONFIDENTIAL

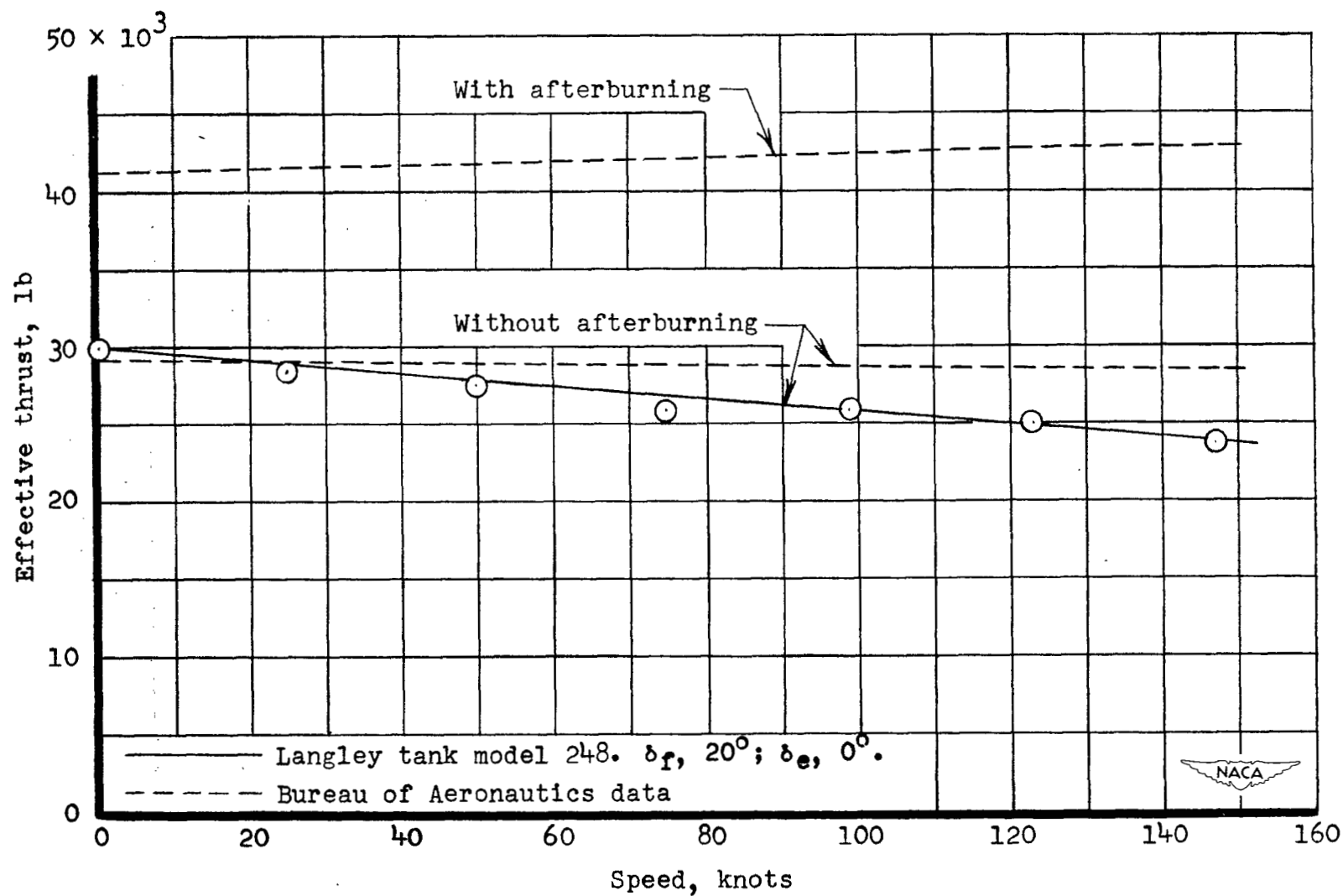


Figure 7.- Effective thrust.

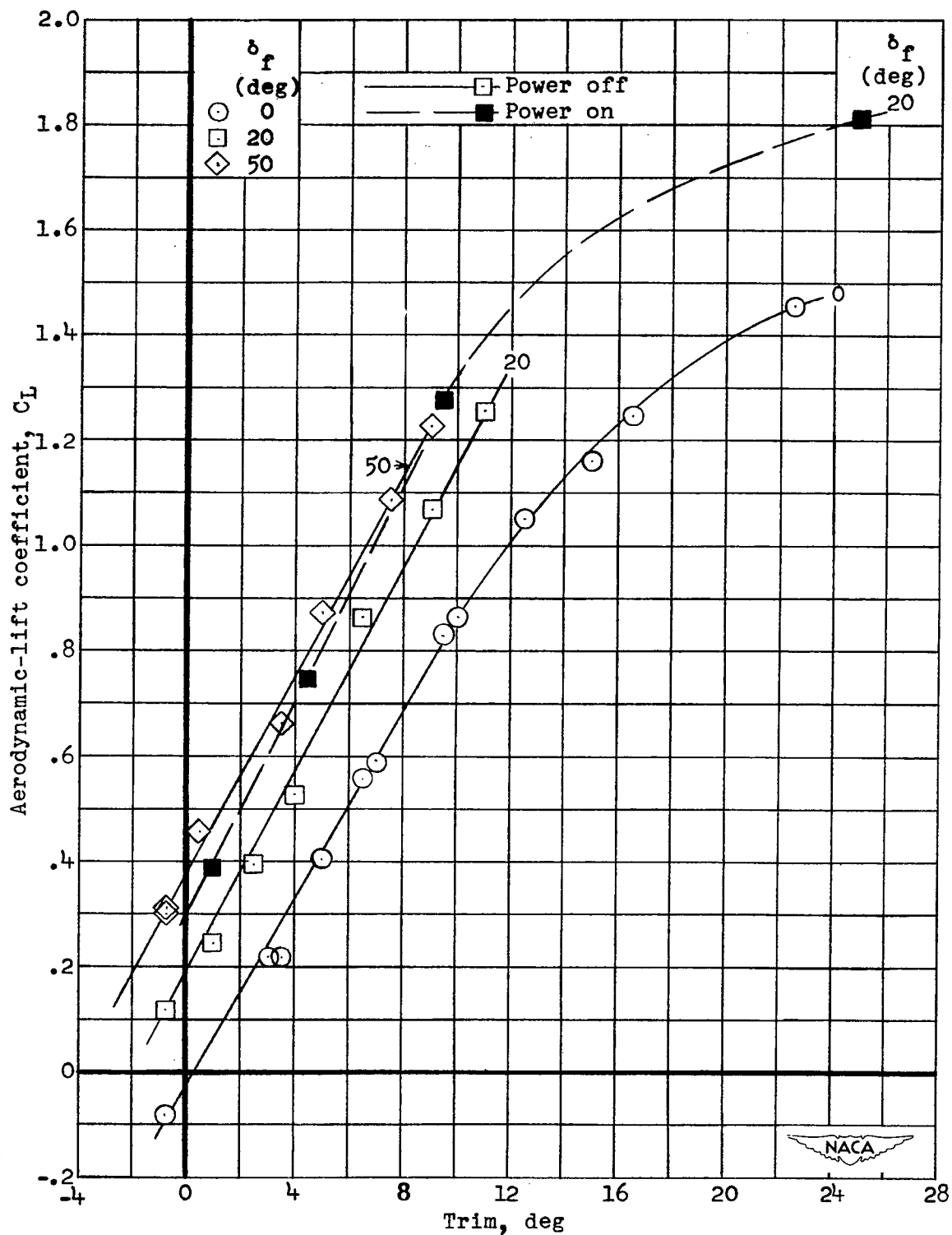


Figure 8.- Aerodynamic-lift coefficient.

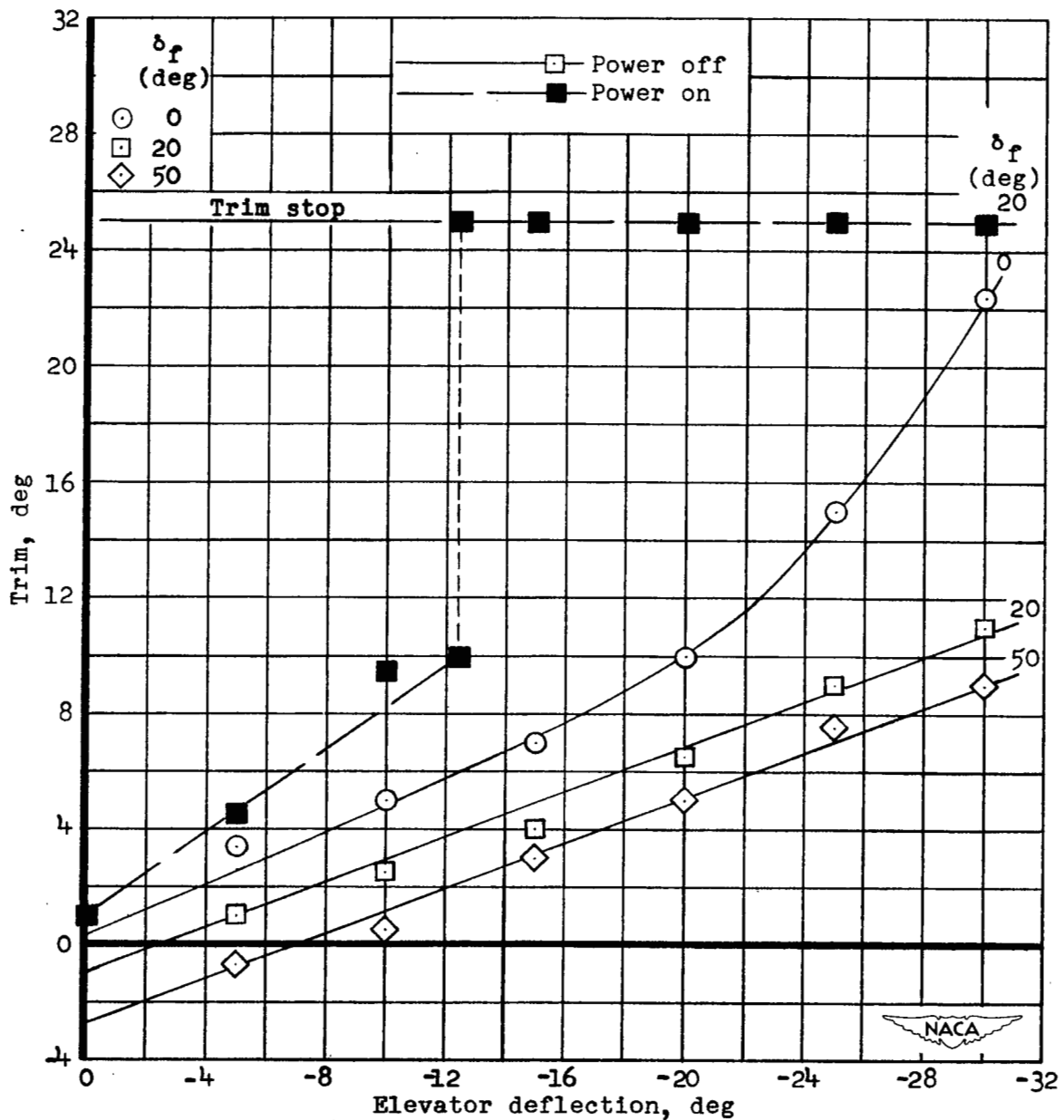
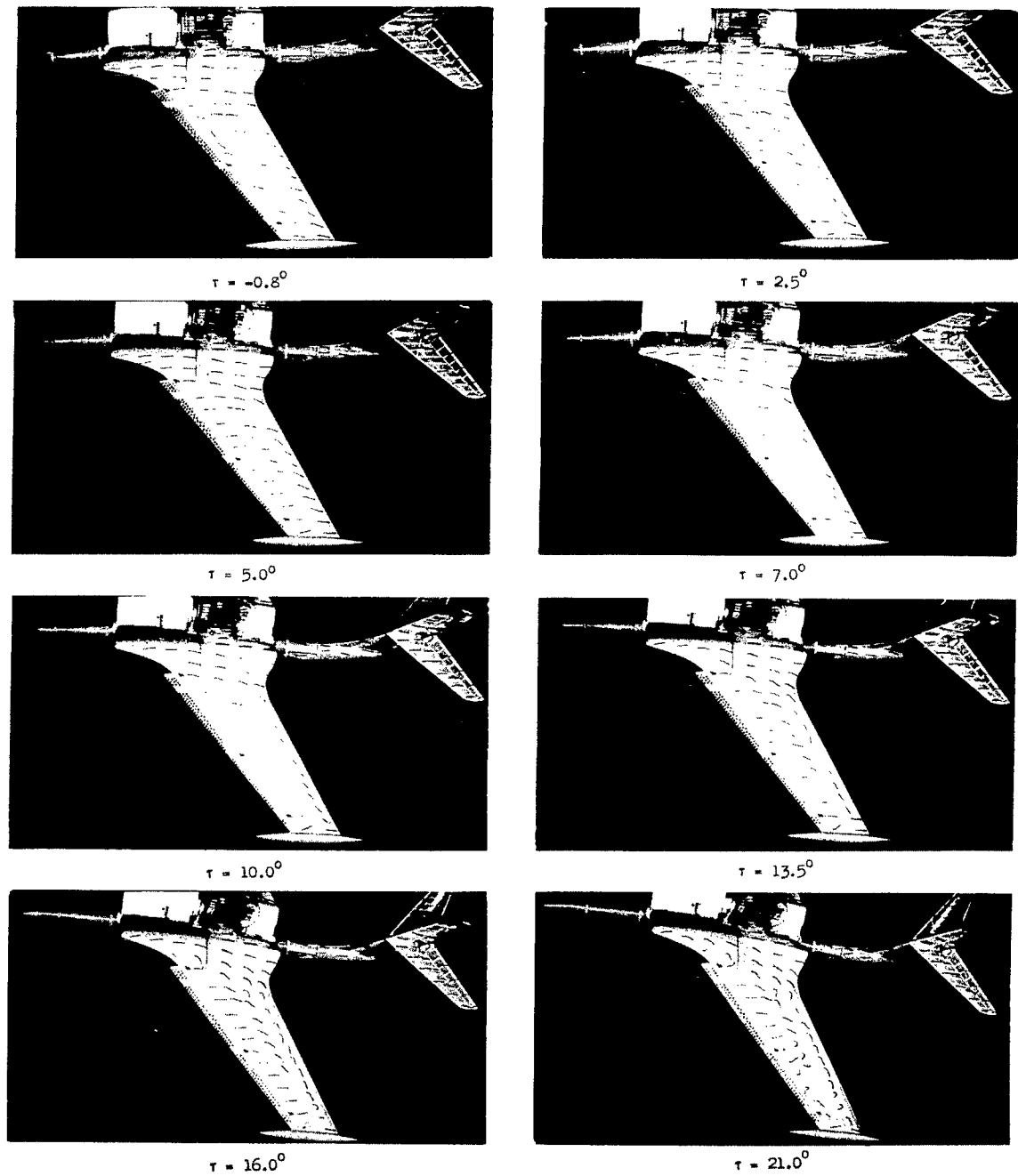
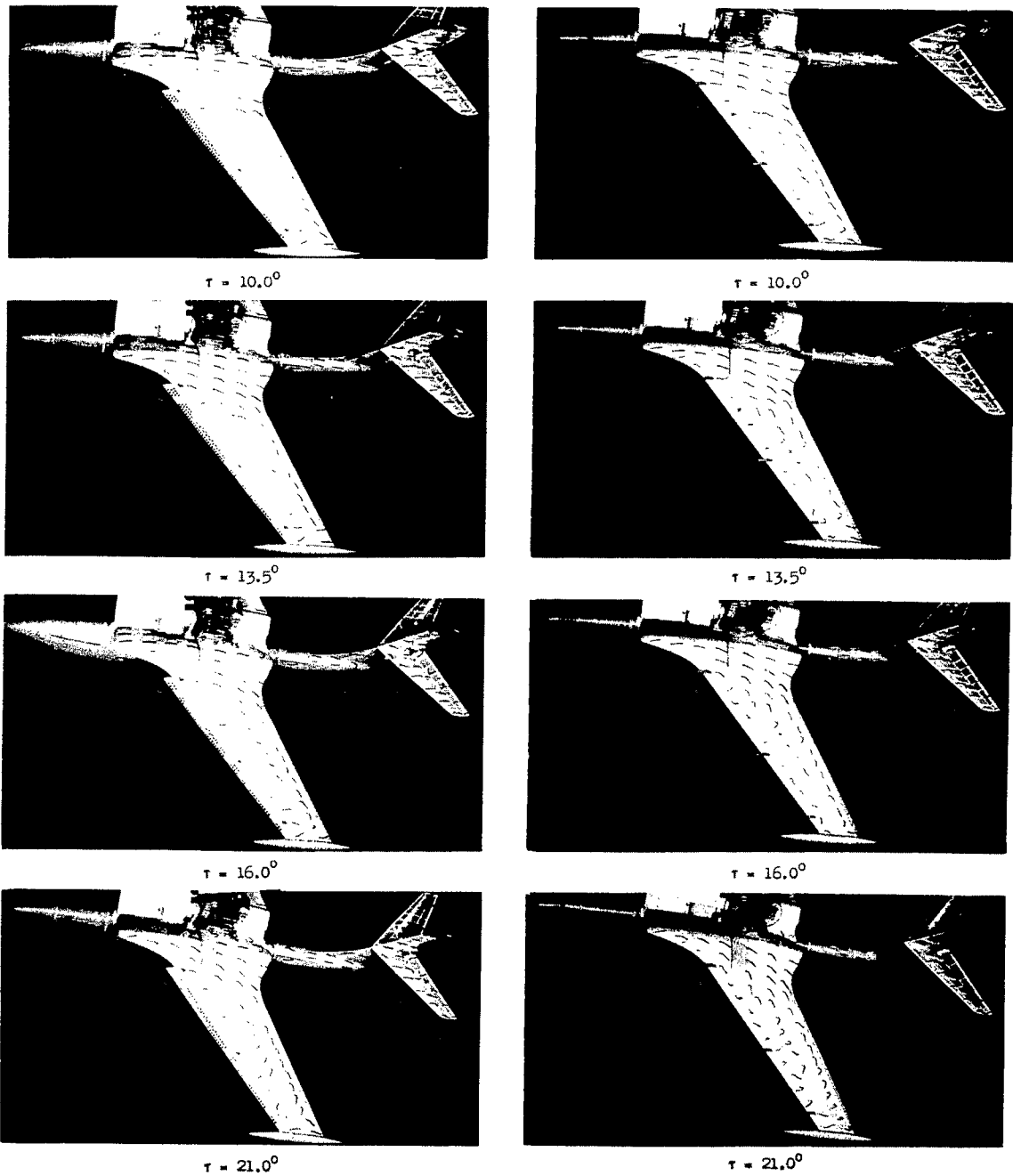


Figure 9.- Variation of trim with elevator deflection. Center-of-gravity location, 26 percent mean aerodynamic chord.



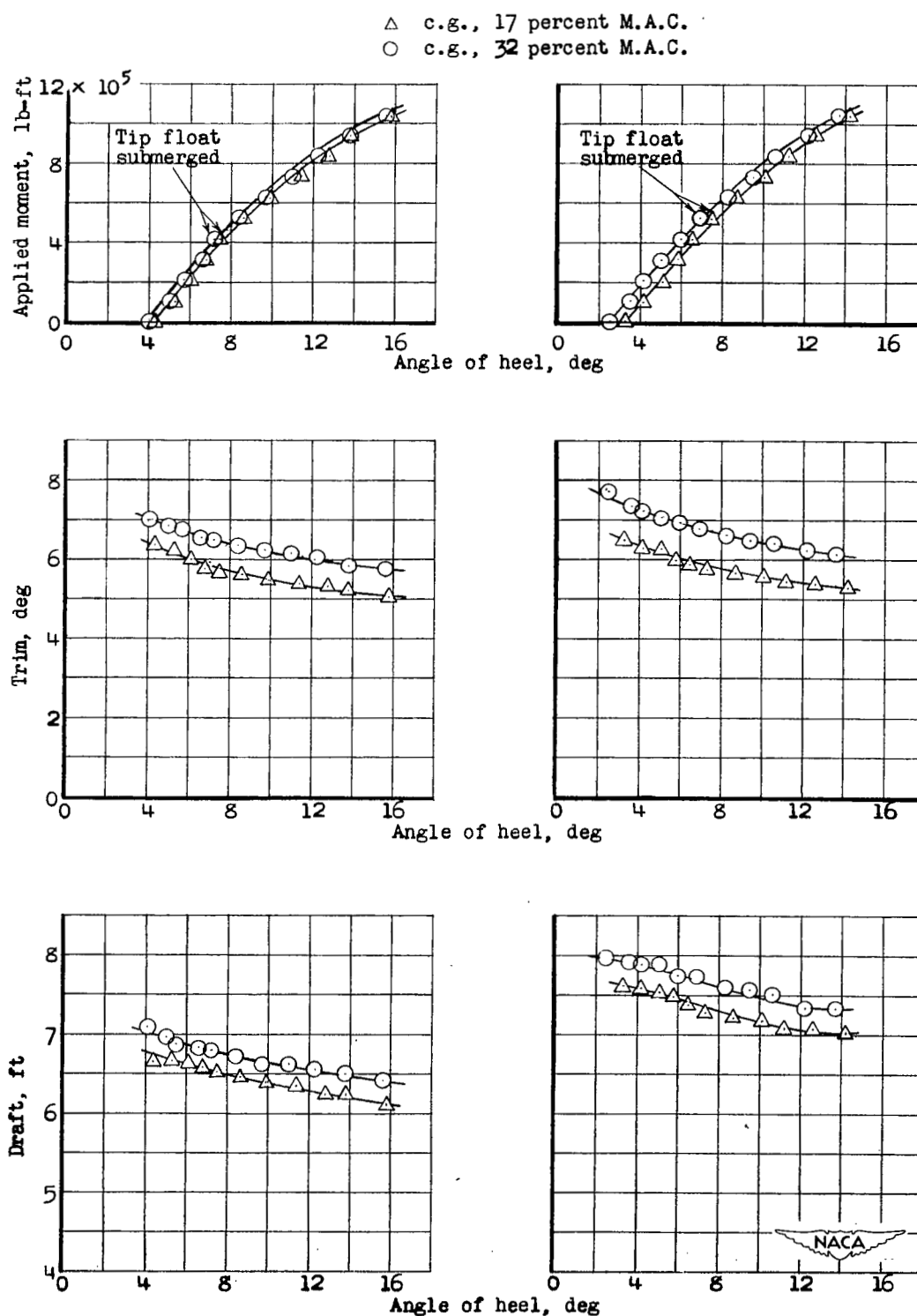
NACA
L-68413

Figure 10.- Tuft studies of air flow over wing, hull, and tail surfaces.
Power on; V, 110 knots.



NACA
L-68414

Figure 11.- Tuft studies of air flow over slotted and unslotted wing.
Power off; V, 110 knots.



(a) Gross load = 95,000 pounds. (b) Gross load = 130,000 pounds.

Figure 12.- Static properties.

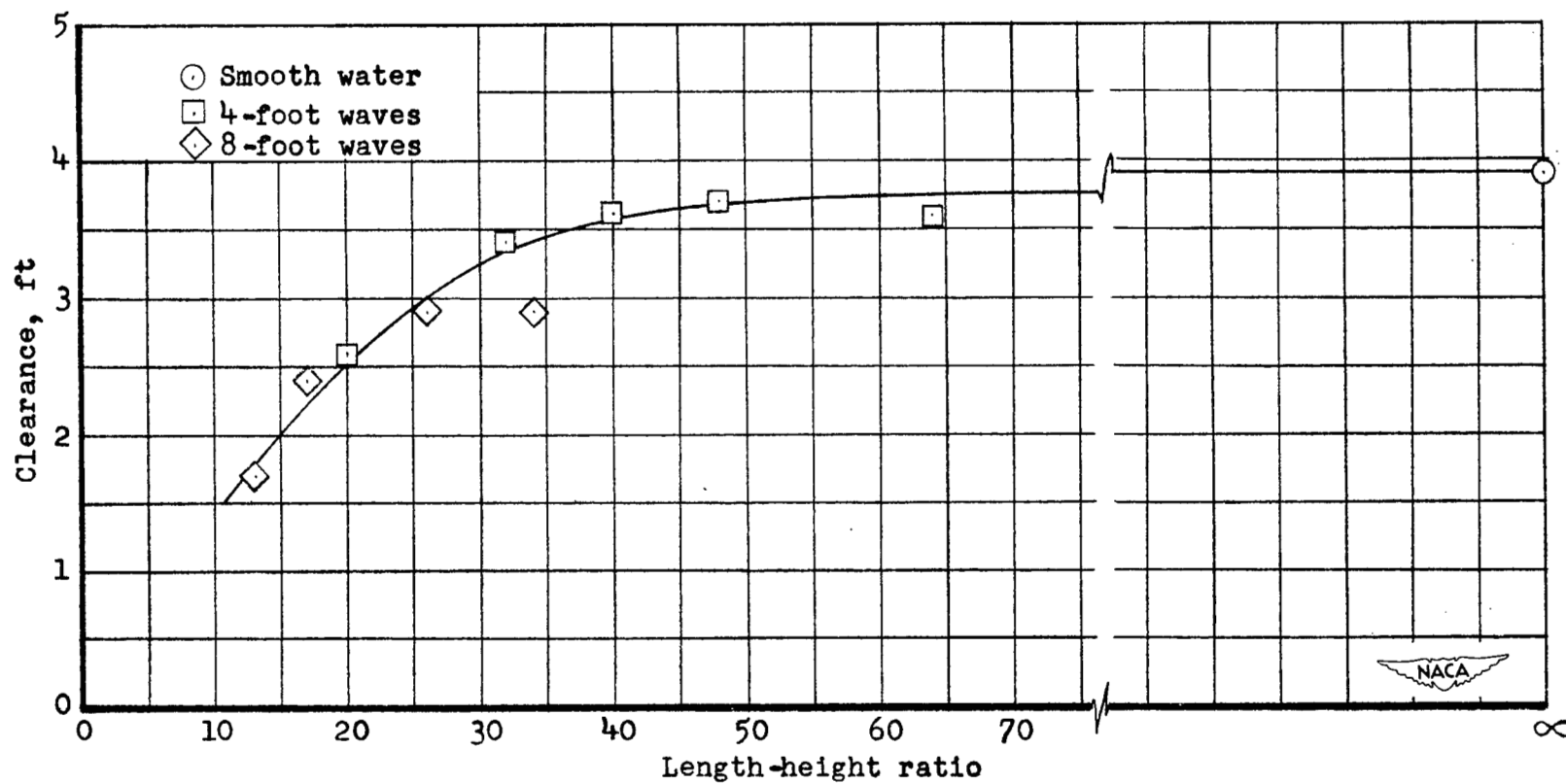


Figure 13.- Jet exit clearance. Δ_0 , 130,000 pounds; center-of-gravity location, 24 percent mean aerodynamic chord.

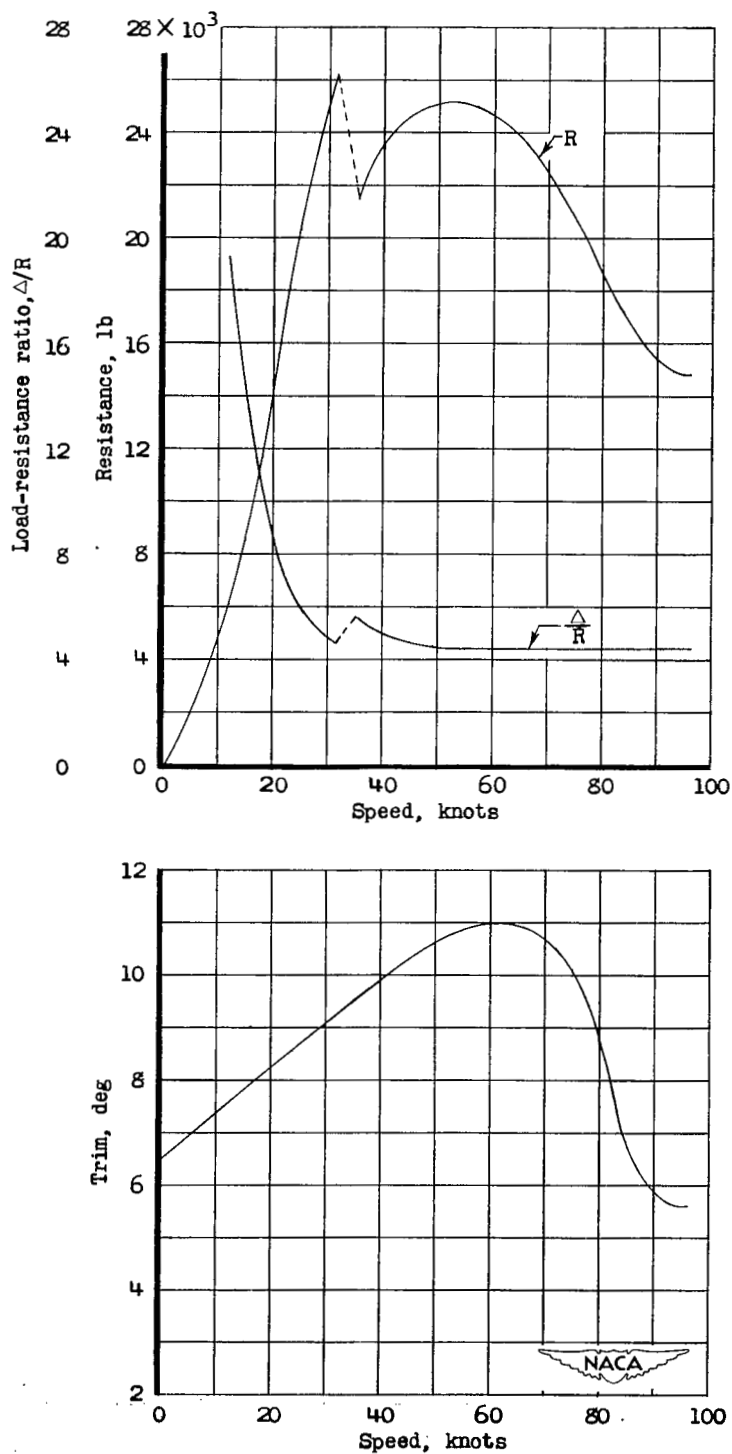


Figure 14.- Minimum resistance, load-resistance ratio, and best trim of hull with wing removed. Δ_0 , 130,000 pounds.

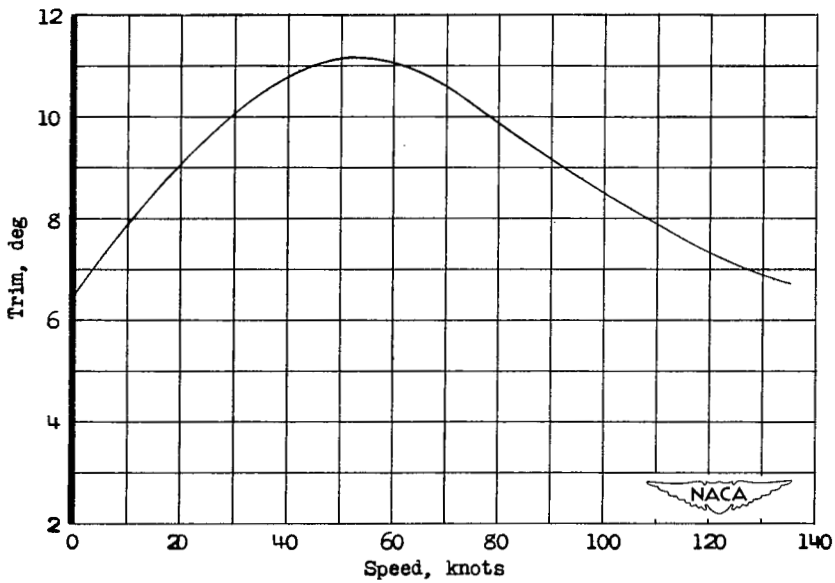
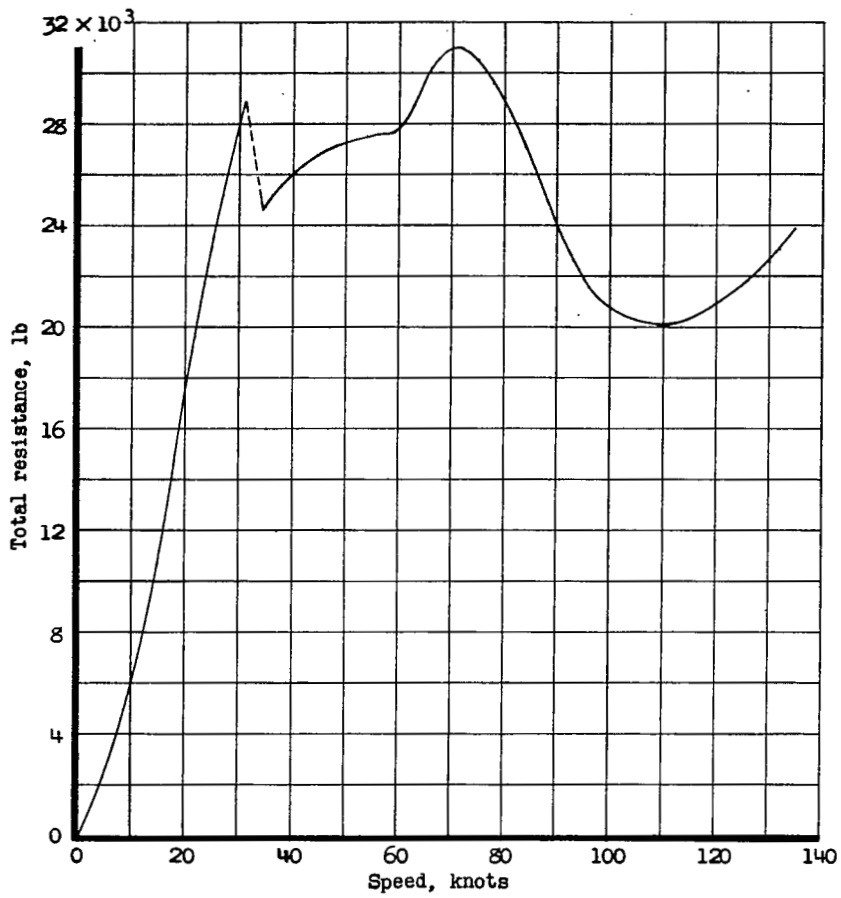


Figure 15.- Minimum total resistance and best trim. Δ_0 , 130,000 pounds;
 δ_f , 20° .

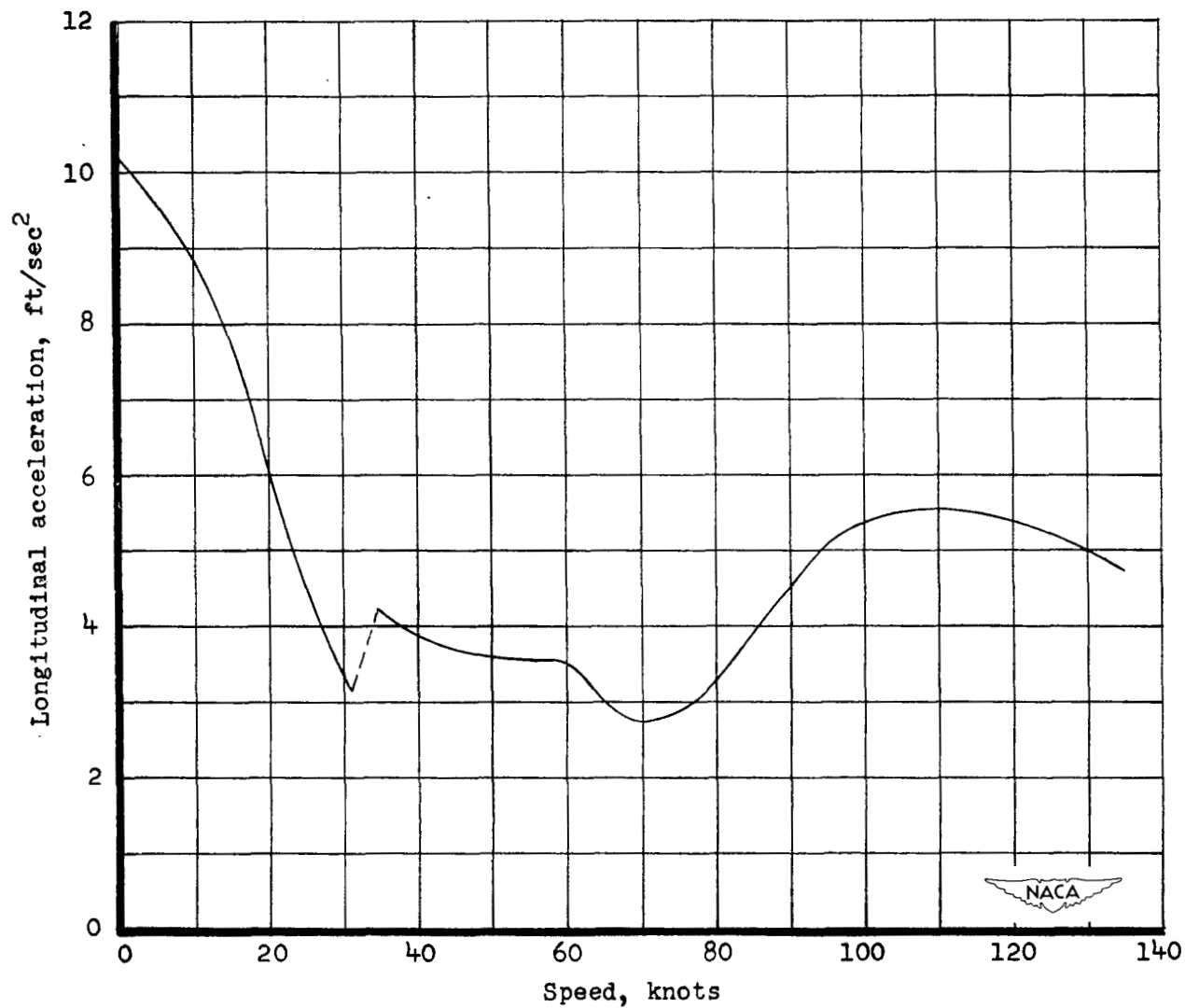
~~CONFIDENTIAL~~

Figure 16.- Longitudinal acceleration for take-off with afterburning.
 Δ_0 , 130,000 pounds; δ_f , 20°.

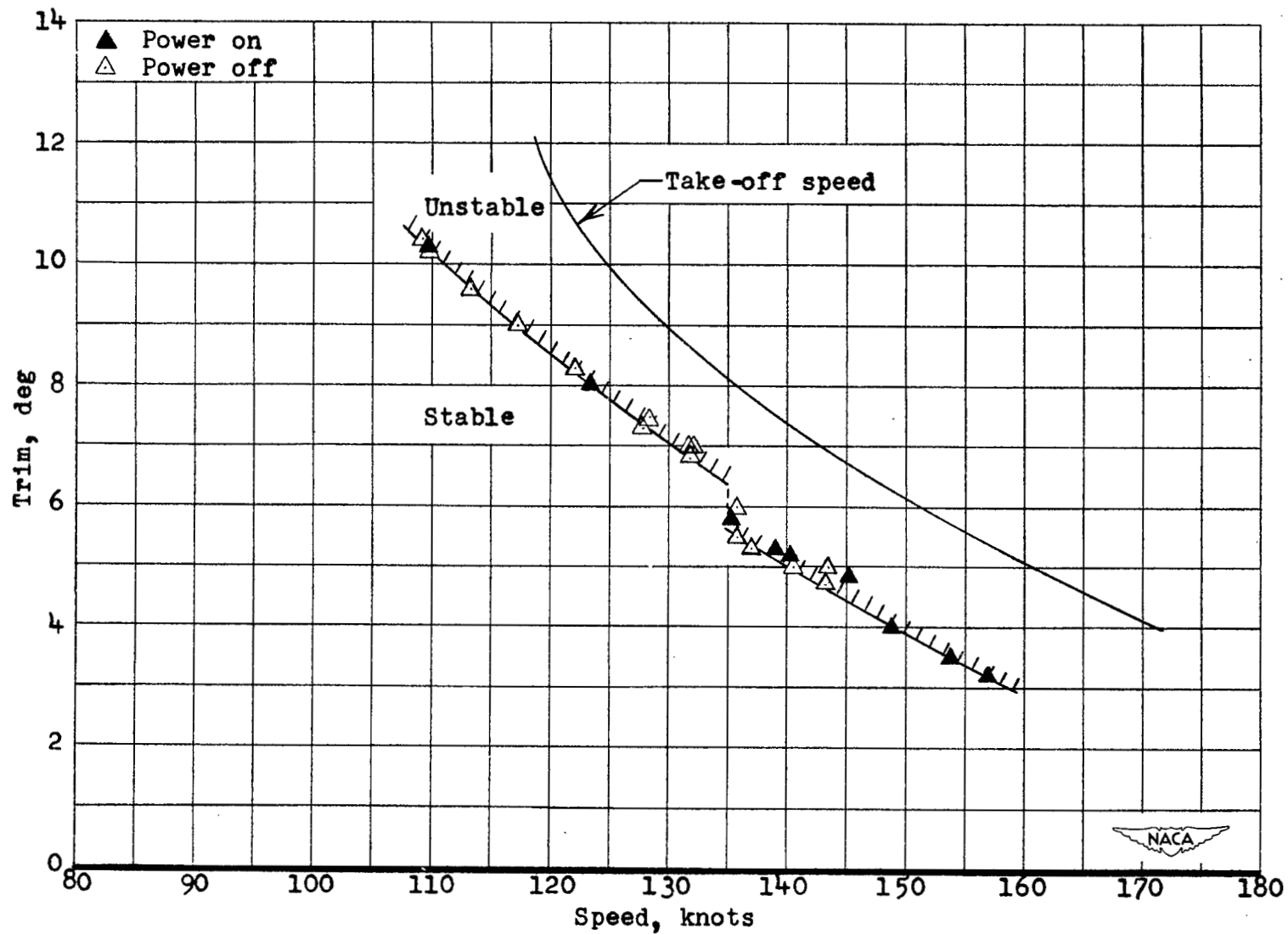
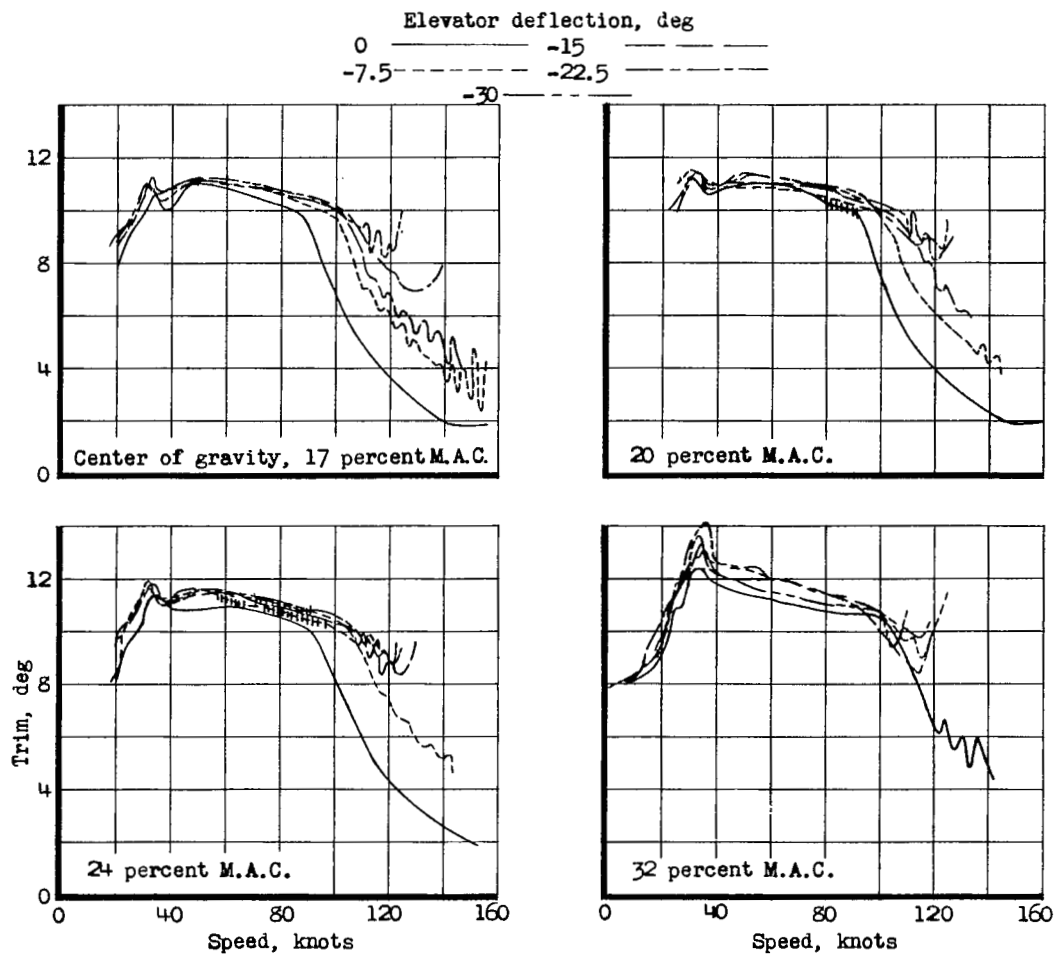
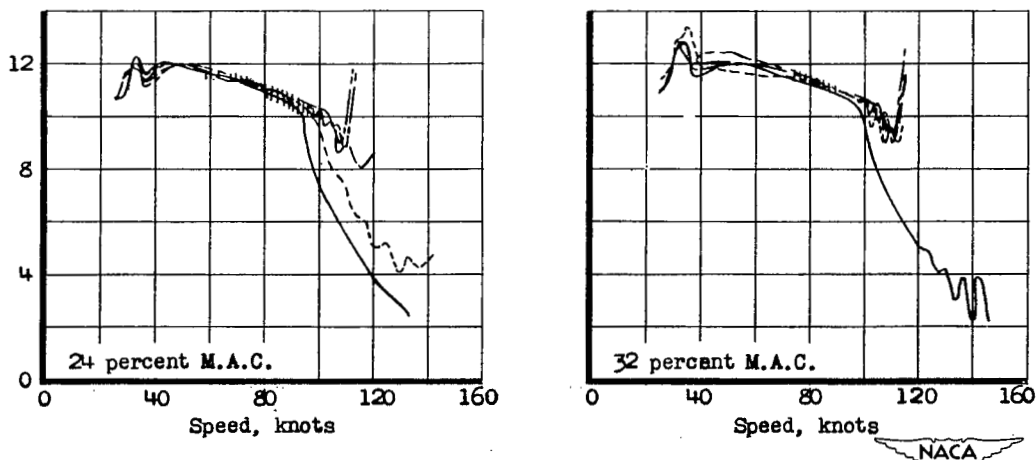


Figure 17.- Trim limits of stability. Δ_0 , 130,000 pounds; δ_F , 20° .

(a) Flap deflection, 20° .(b) Flap deflection, 50° .Figure 18.- Representative trim tracks during take-off. Δ_0 , 130,000 pounds.

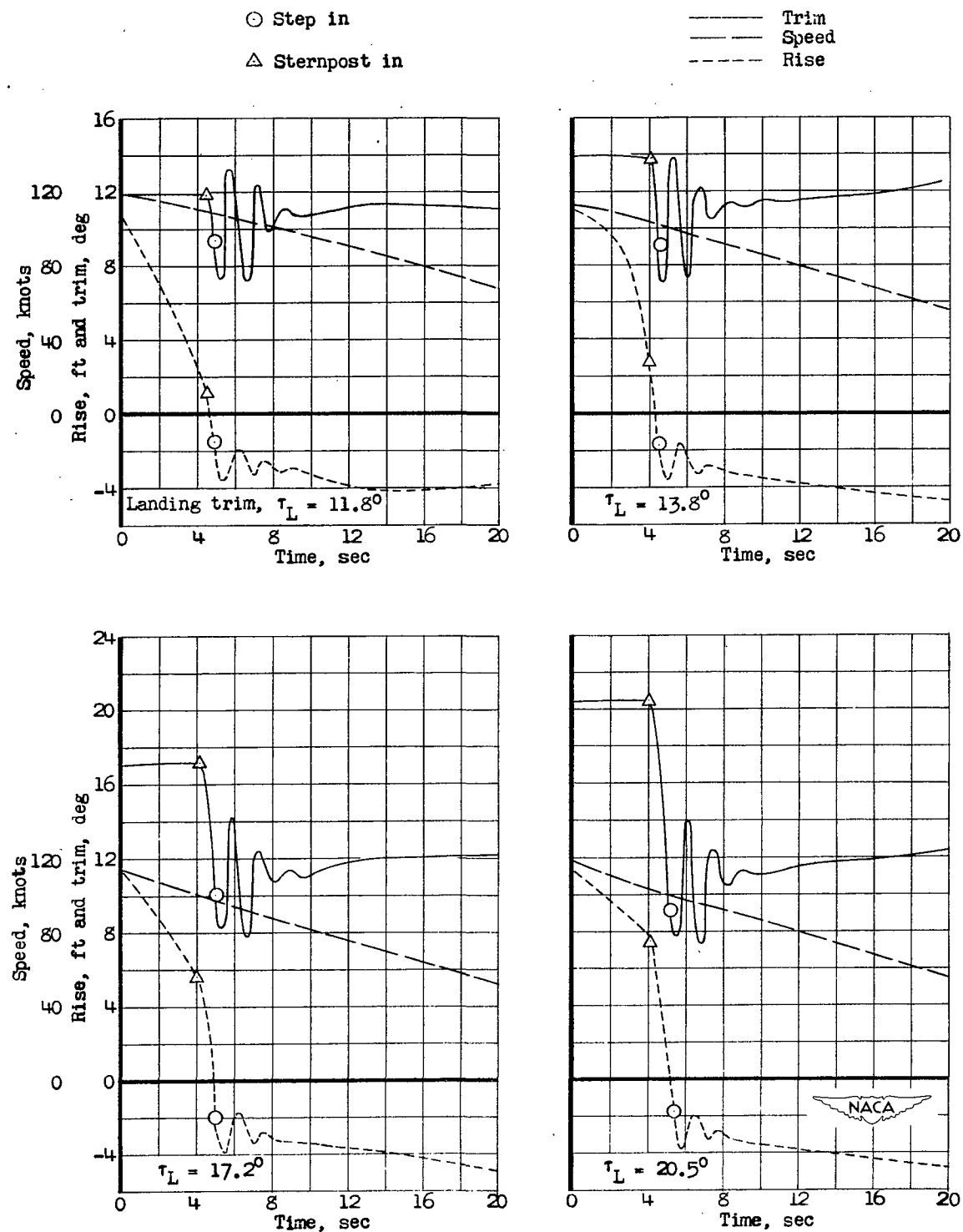
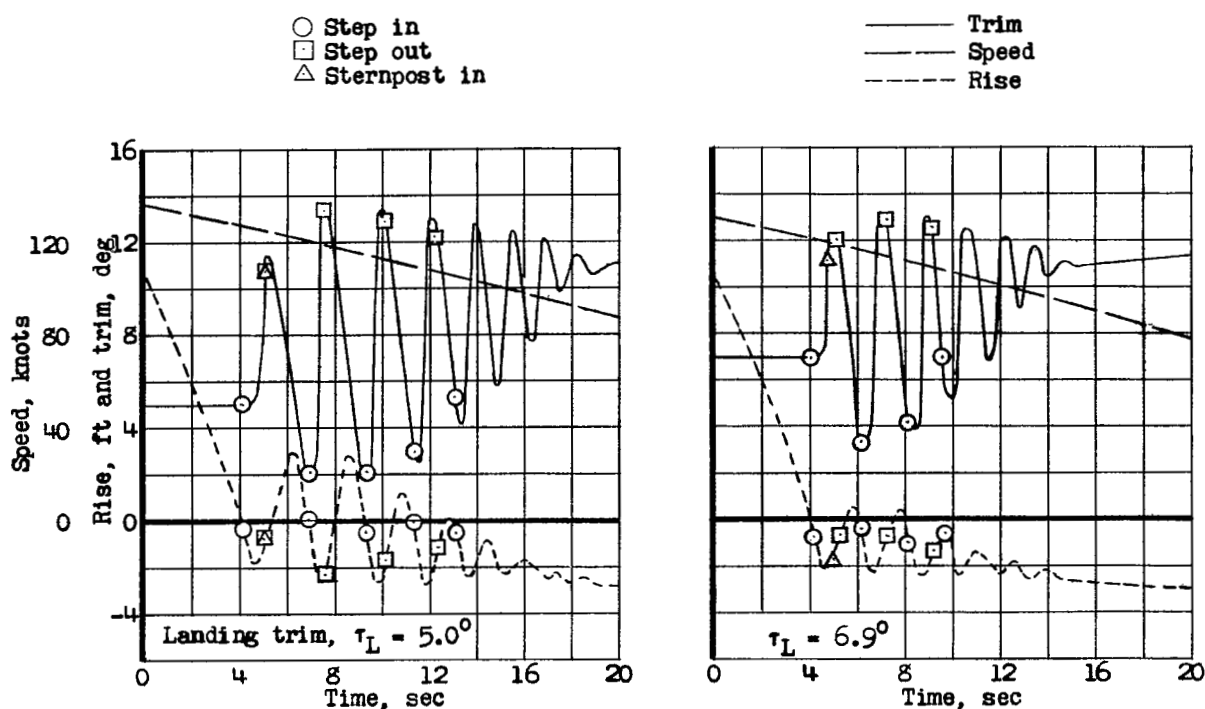
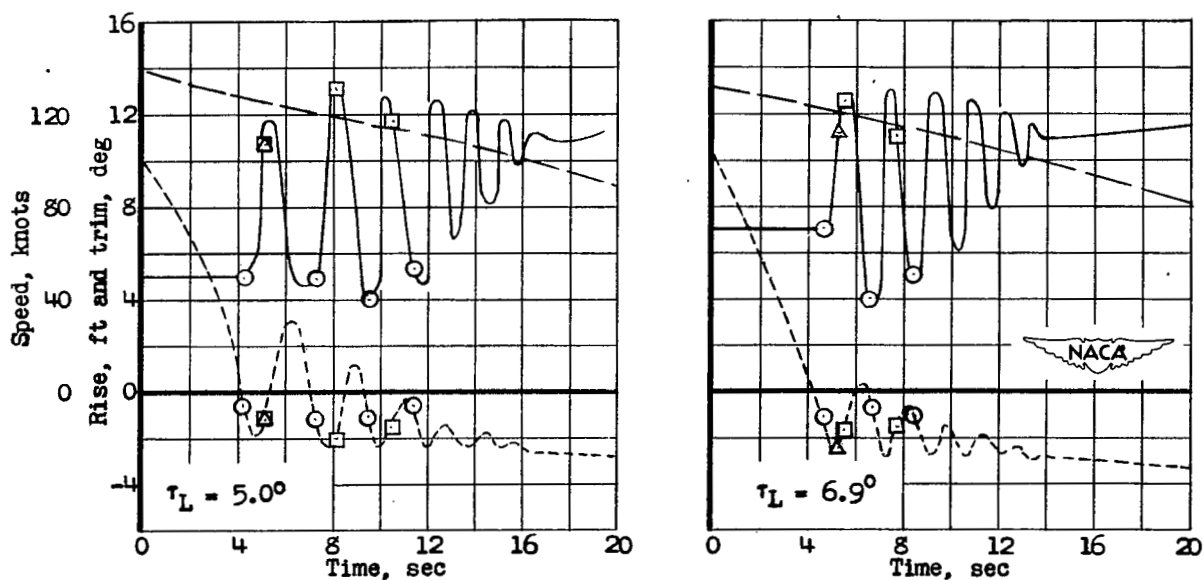


Figure 19.- Typical time histories of landings in smooth water. Δ_0 , 130,000 pounds; δ_f , 50° ; center-of-gravity location, 32 percent mean aerodynamic chord.



(a) Center-of-gravity location, 20 percent mean aerodynamic chord.



(b) Center-of-gravity location, 32 percent mean aerodynamic chord.

Figure 20.- Effect of center-of-gravity location on landing behavior in smooth water. Δ_0 , 130,000 pounds; δ_F , 50° .

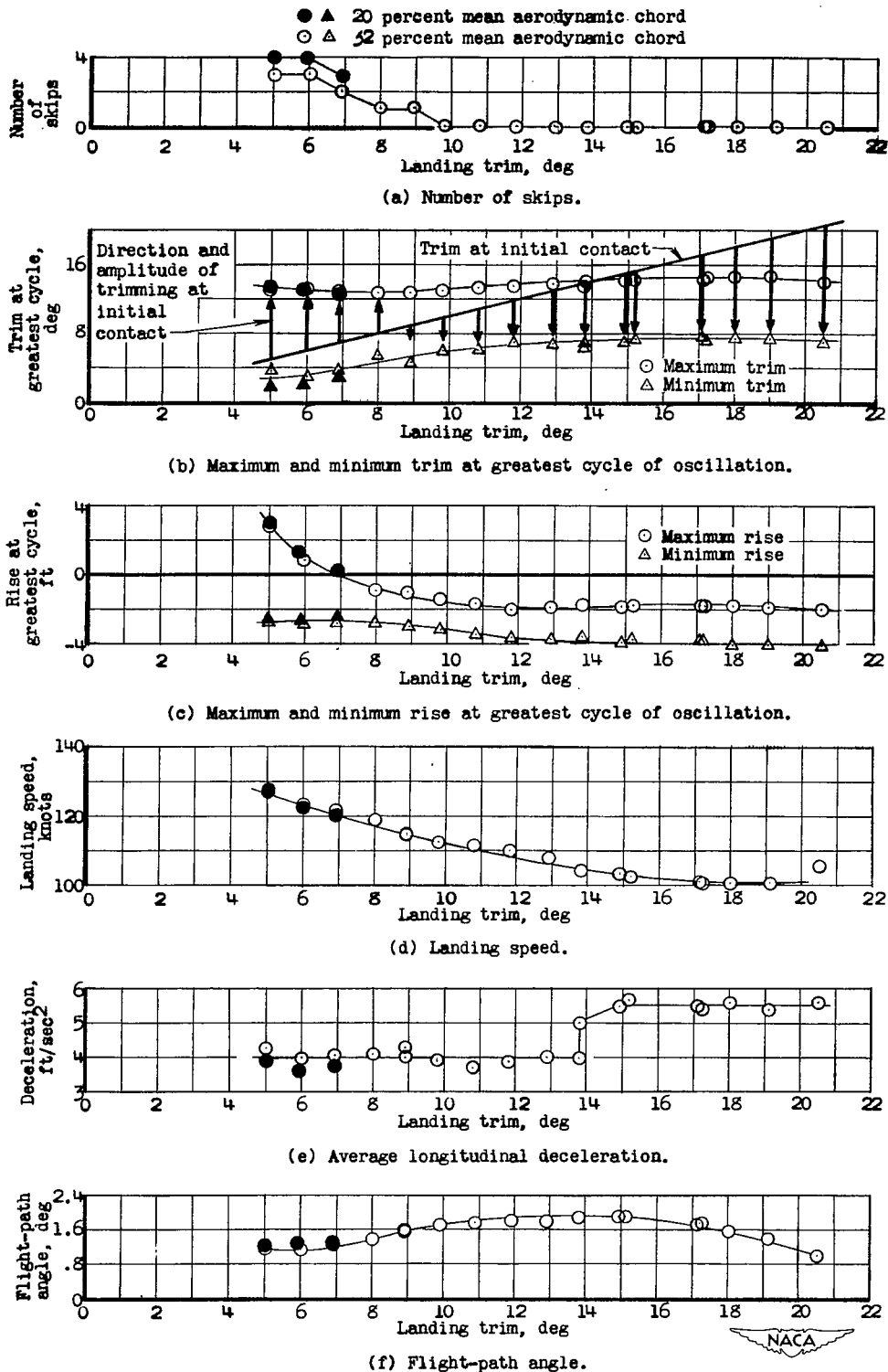


Figure 21.- Landing-stability characteristics in smooth water. Δ_0 , 130,000 pounds; δ_F , 50° .

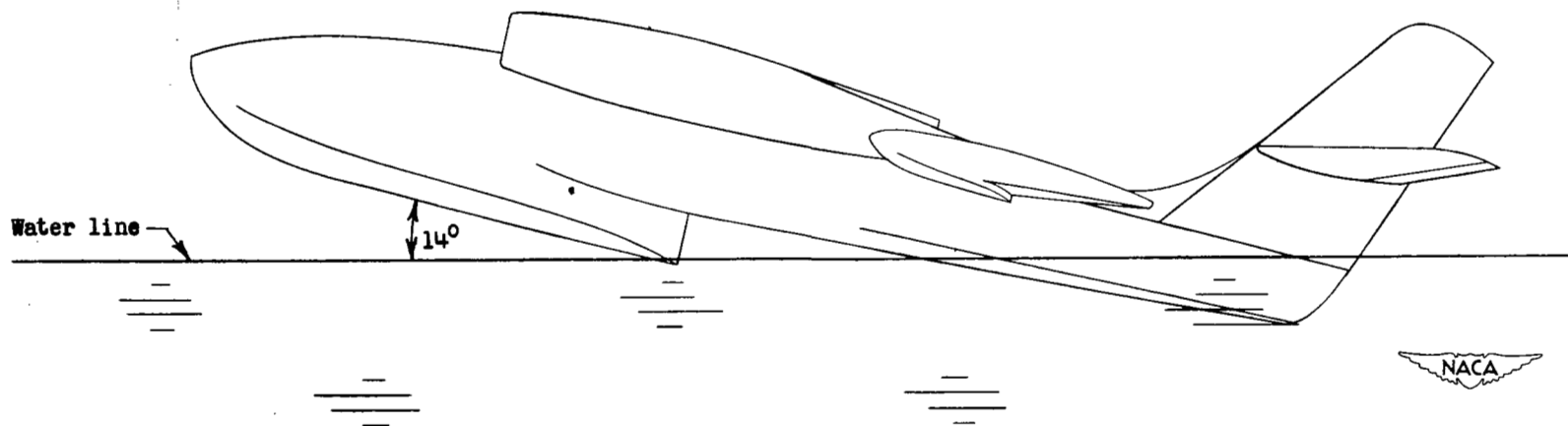


Figure 22.- Attitude of model at a trim of 14° during landings in smooth water.

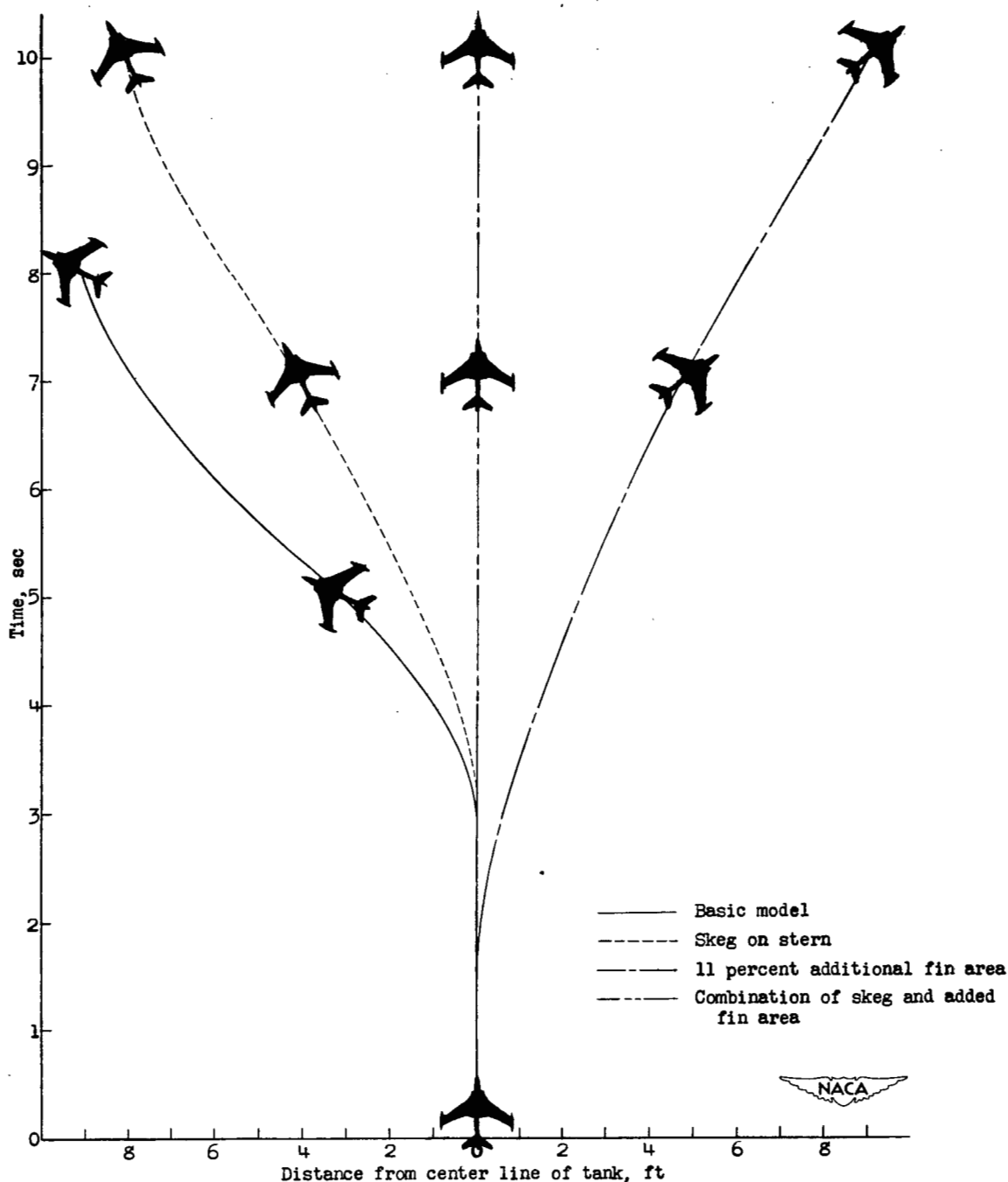


Figure 23.- Typical paths of model during free-body landings in smooth water. Δ_0 , 130,000 pounds; δ_f , 50° ; center-of-gravity location, 28 percent mean aerodynamic chord; τ_L , 12° .

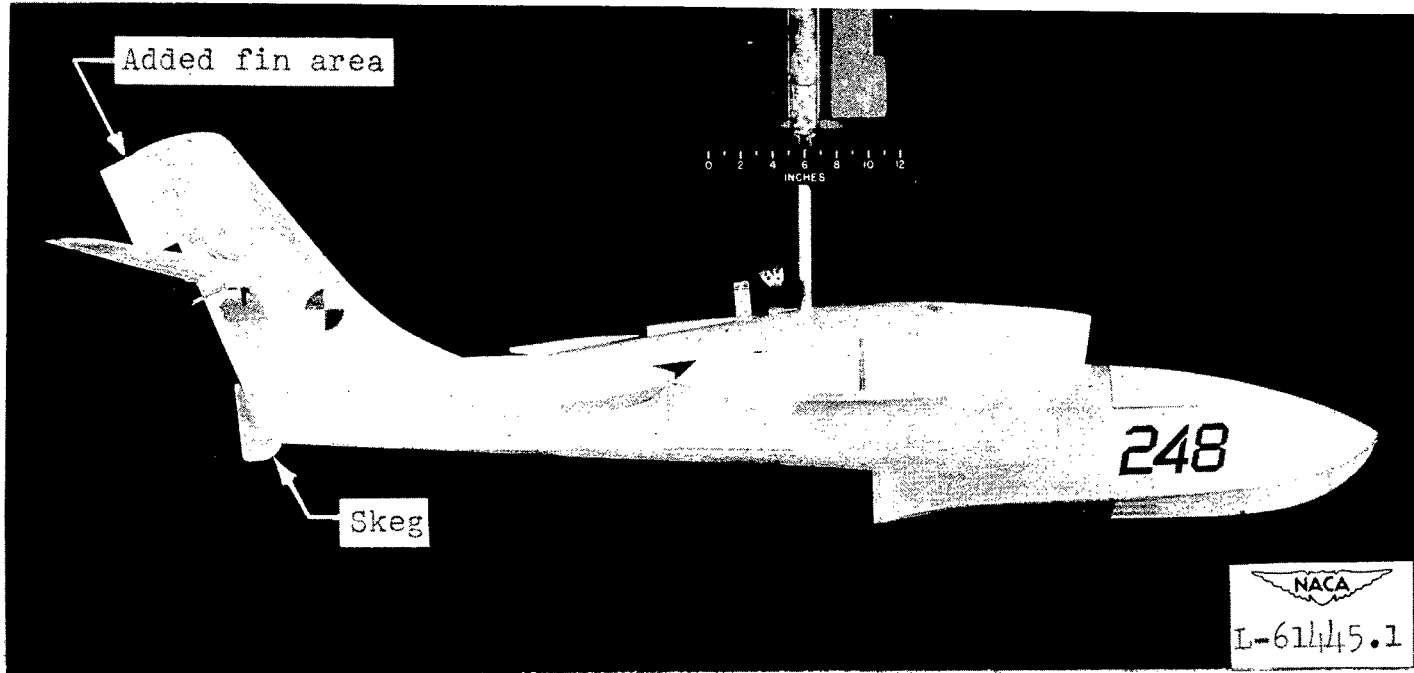


Figure 24.- Langley tank model 248 with skeg and added fin area.

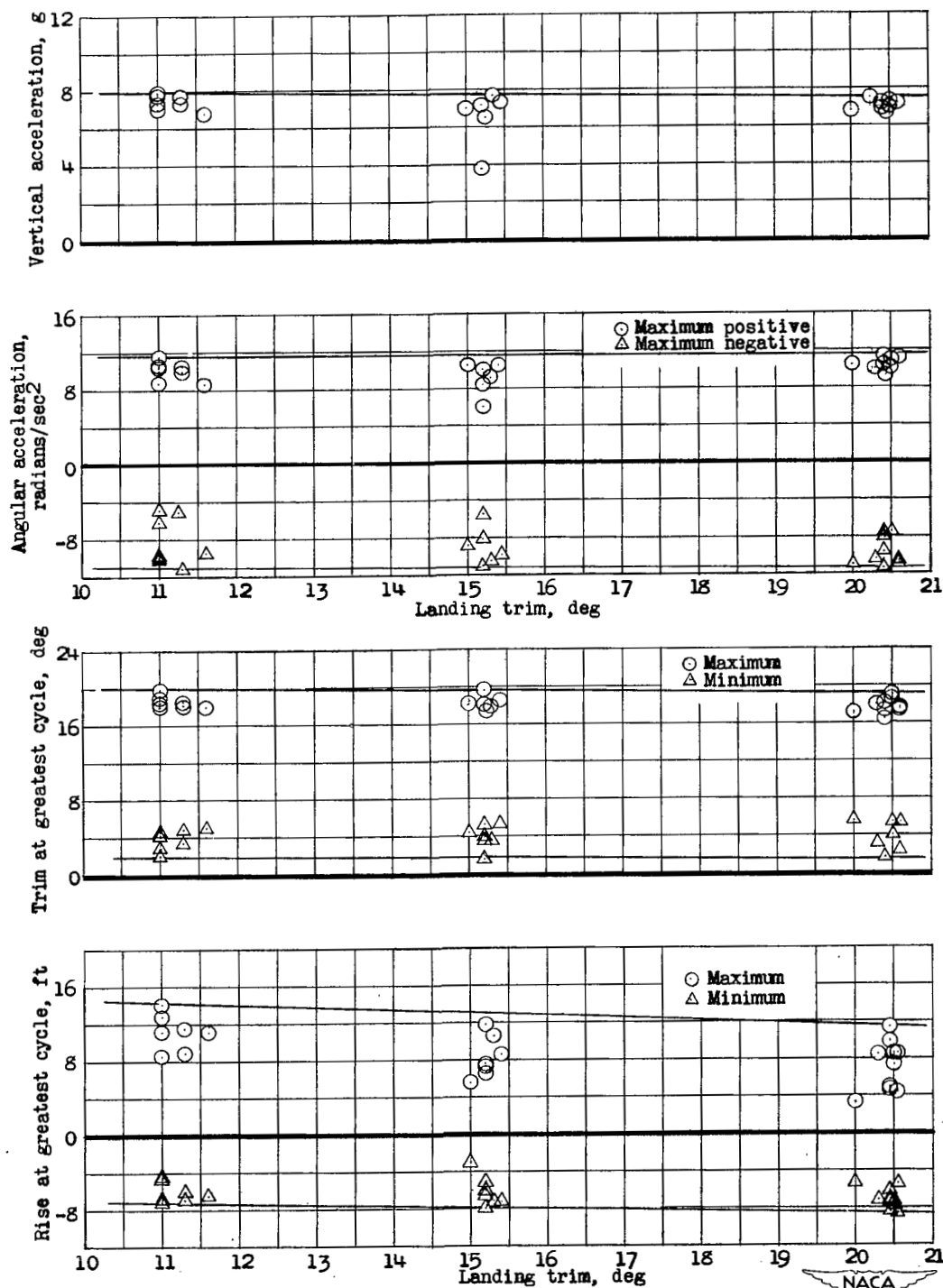


Figure 25.- Effect of landing trim on rough-water behavior. Δ_0 , 117,000 pounds; δ_F , 50° ; center-of-gravity location, 28 percent mean aerodynamic chord; waves, 8 feet high and 340 feet long.

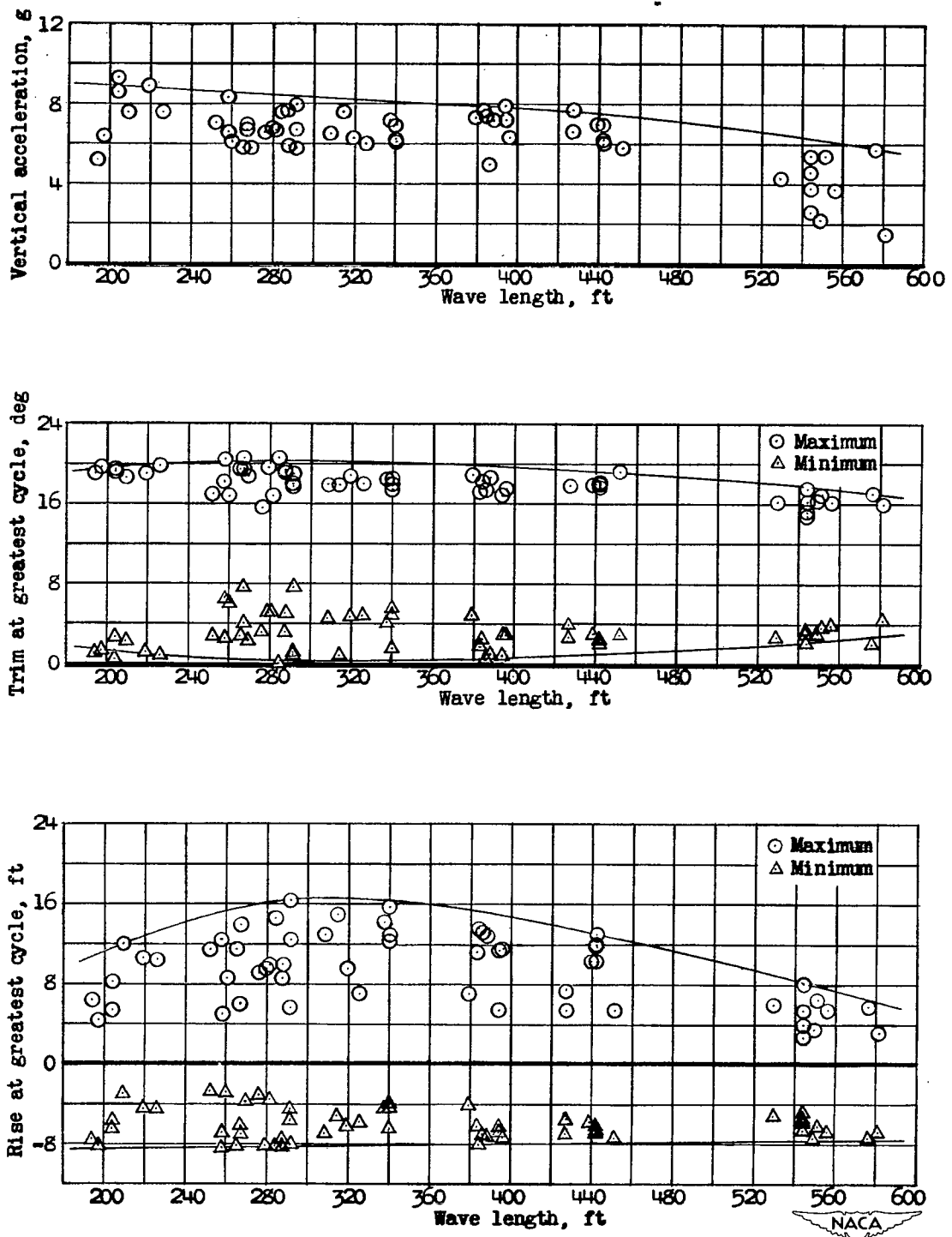


Figure 26.- Effect of wave length on rough-water landings. Δ_0 , 110,000 pounds; δ_f , 50° ; center-of-gravity location, 28 percent mean aerodynamic chord; τ_L , 12° ; waves, 8 feet high.

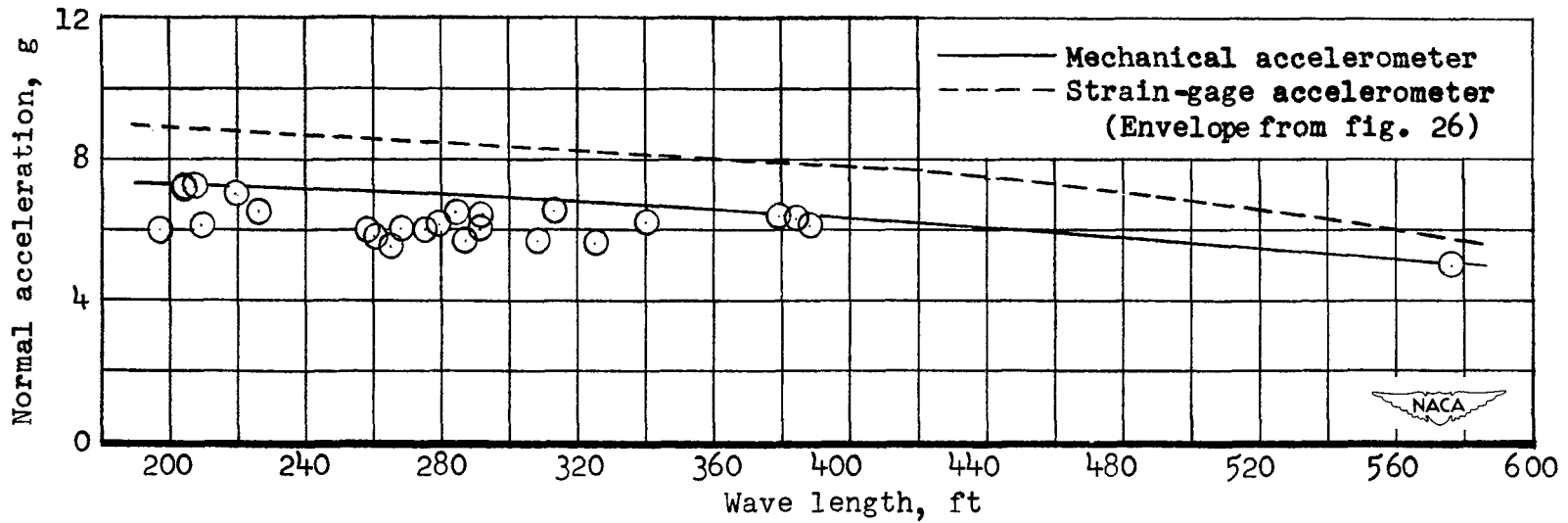


Figure 27.- Accelerations normal to keel during rough-water landings with fore-and-aft gear. Δ_0 , 110,000 pounds; δ_f , 50° ; center-of-gravity location, 28 percent mean aerodynamic chord; τ_L , 12° ; waves, 8 feet high.

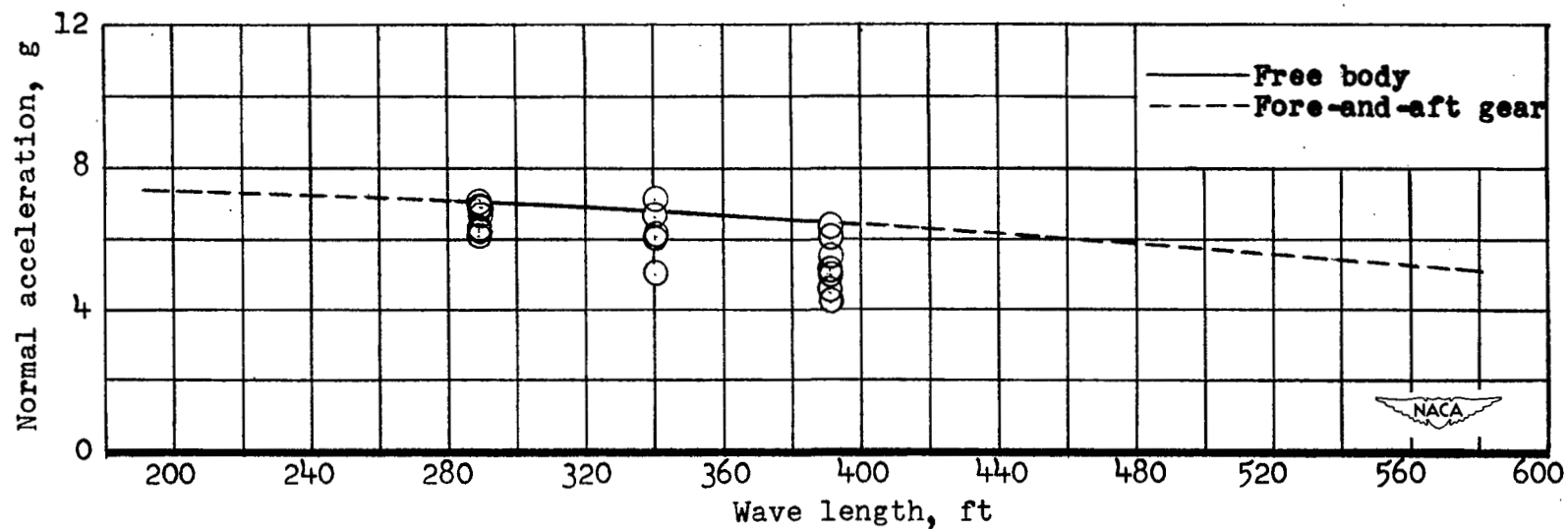


Figure 28.- Accelerations normal to keel during free-body landings in rough water. Δ_0 , 110,000 pounds; δ_F , 50° ; center-of-gravity location, 28 percent mean aerodynamic chord; τ_L , 12° ; waves, 8 feet high.

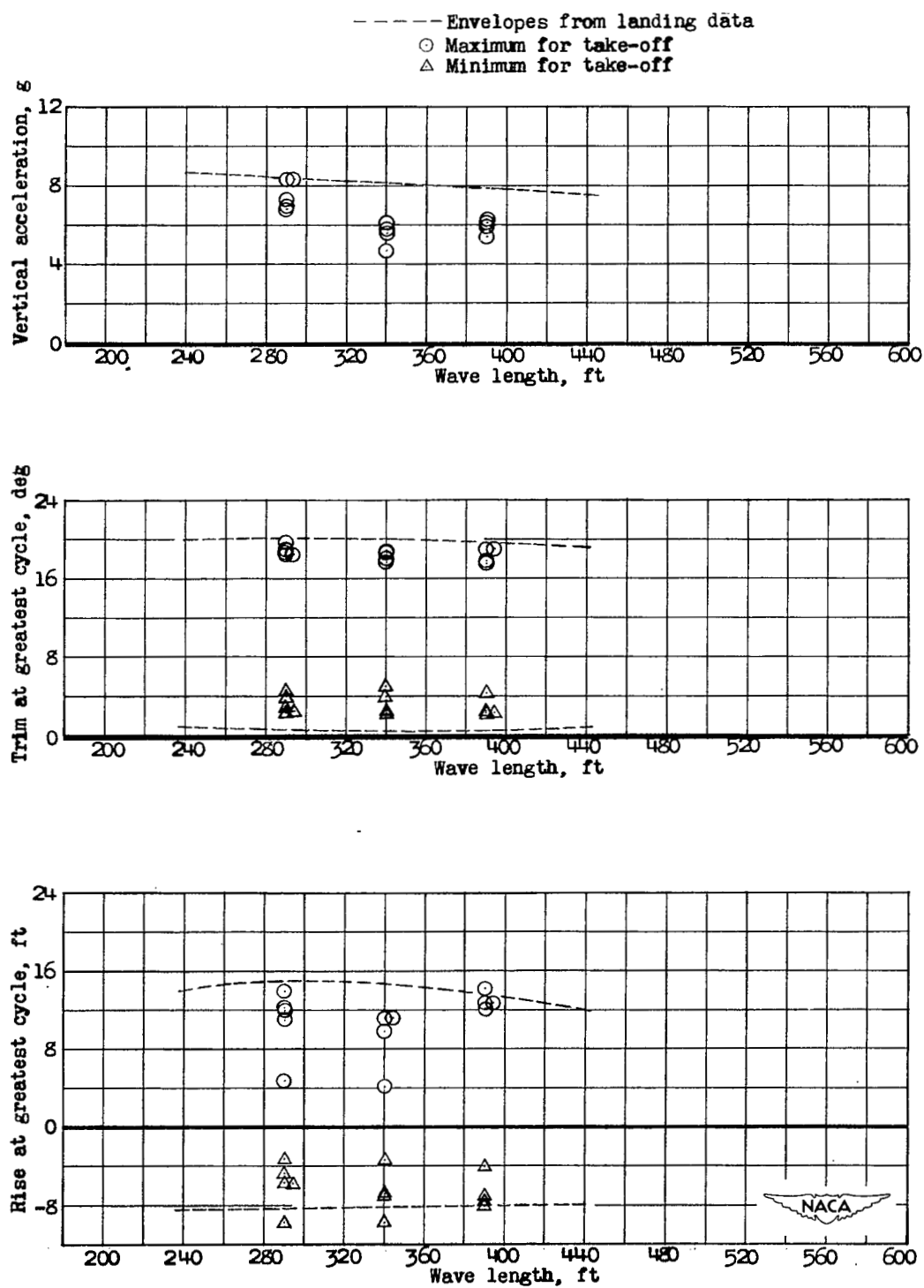
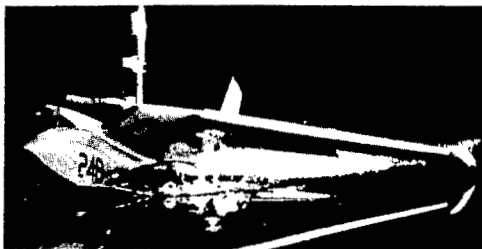


Figure 29.- Effect of wave length on rough-water take-offs. Δ_0 , 130,000 pounds; δ_F , 50° ; center-of-gravity location, 28 percent mean aerodynamic chord; waves, 8 feet high.



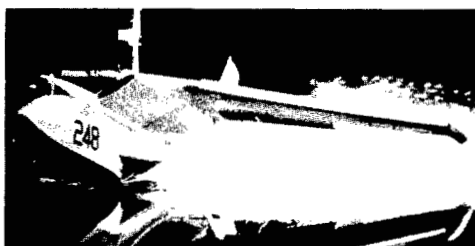
$V = 24.4 \text{ knots}; \tau = 10.0^\circ$



$V = 73.2 \text{ knots}; \tau = 11.5^\circ$



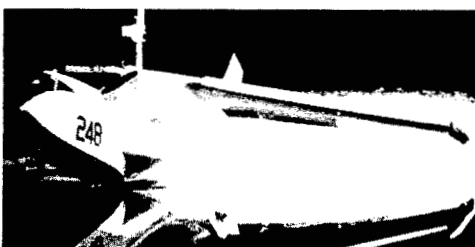
$V = 36.6 \text{ knots}; \tau = 11.5^\circ$



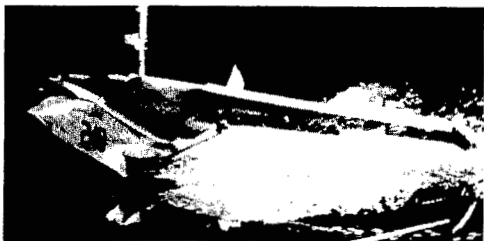
$V = 85.4 \text{ knots}; \tau = 11.0^\circ$



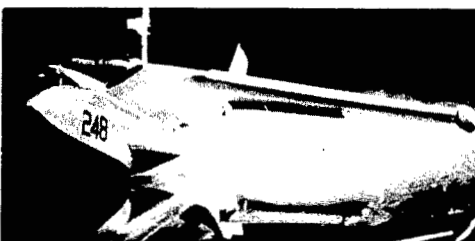
$V = 48.8 \text{ knots}; \tau = 12.0^\circ$



$V = 97.6 \text{ knots}; \tau = 10.5^\circ$



$V = 61.0 \text{ knots}; \tau = 12.0^\circ$

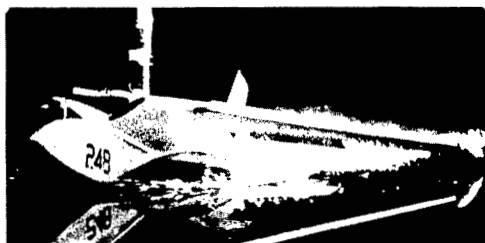


$V = 109.8 \text{ knots}; \tau = 10.0^\circ$



L-68415

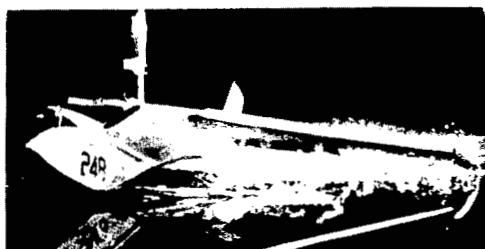
Figure 30.- Forebody spray during take-off. Power on; Δ_0 , 130,000 pounds; δ_f , 20° ; δ_e , -10° ; center-of-gravity location, 28 percent mean aerodynamic chord.



$V = 26.8$ knots; $\tau = 10.5^\circ$



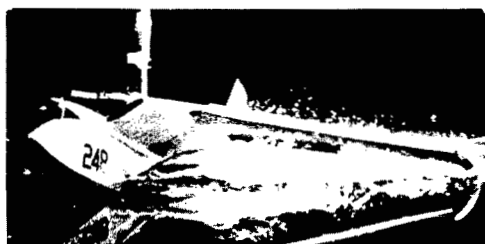
$V = 36.6$ knots; $\tau = 11.5^\circ$



$V = 29.3$ knots; $\tau = 11.5^\circ$



$V = 39.0$ knots; $\tau = 12.0^\circ$



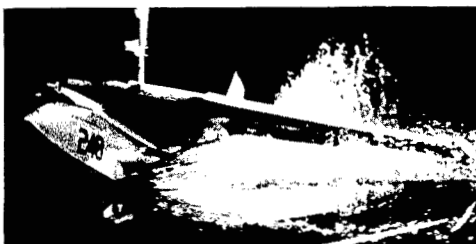
$V = 31.7$ knots; $\tau = 11.5^\circ$



$V = 41.5$ knots; $\tau = 12.0^\circ$



$V = 34.2$ knots; $\tau = 11.5^\circ$



$V = 43.9$ knots; $\tau = 12.0^\circ$

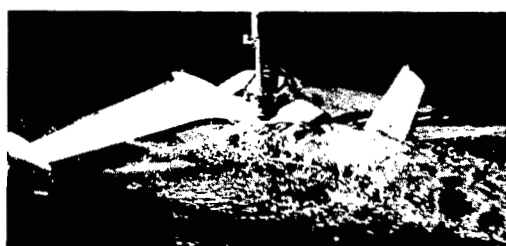


L-68416

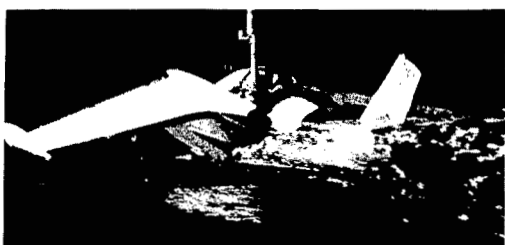
Figure 31.- Spray on flaps during take-off. Power on; Δ_0 , 130,000 pounds; δ_f , 20° ; δ_e , -10° ; center-of-gravity location, 28 percent mean aerodynamic chord.



$V = 109.8 \text{ knots}; \tau = 10.5^\circ$



$V = 61.0 \text{ knots}; \tau = 12.5^\circ$



$V = 97.6 \text{ knots}; \tau = 11.0^\circ$



$V = 48.8 \text{ knots}; \tau = 12.5^\circ$



$V = 85.4 \text{ knots}; \tau = 11.5^\circ$



$V = 36.6 \text{ knots}; \tau = 12.5^\circ$



$V = 73.2 \text{ knots}; \tau = 12.0^\circ$



$V = 24.4 \text{ knots}; \tau = 10.0^\circ$



L-68417

Figure 32.- Spray on tail surfaces during landing. Power off; Δ_0 , 130,000 pounds; δ_f , 50° ; δ_e , -10° ; center-of-gravity location, 28 percent mean aerodynamic chord.

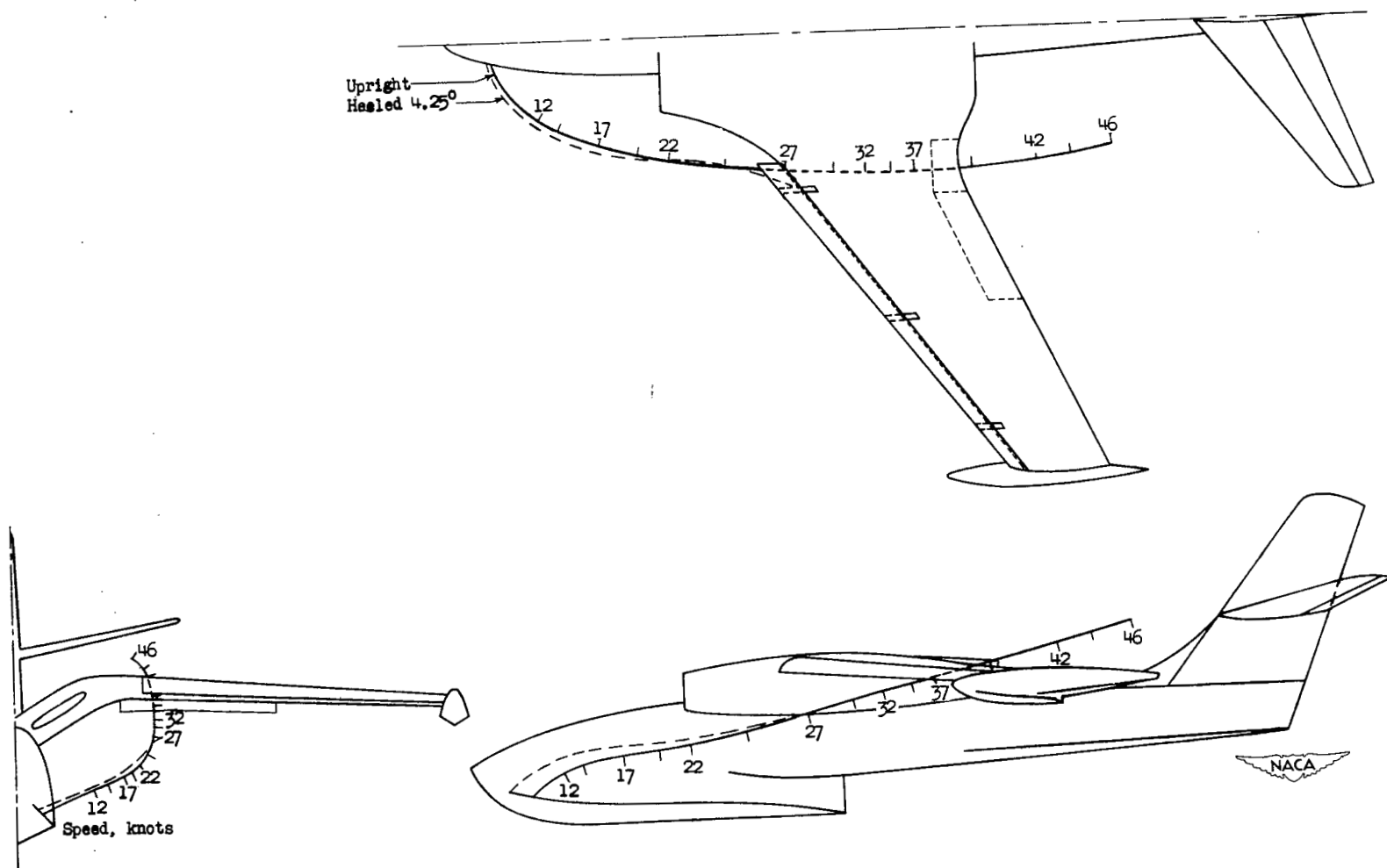
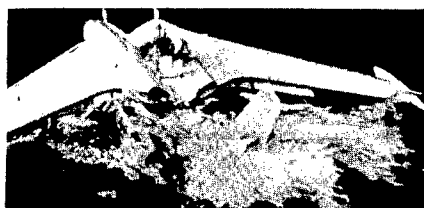
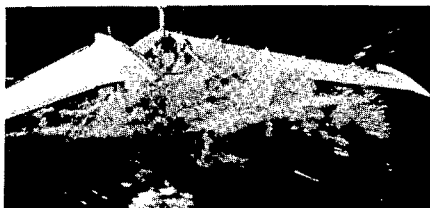
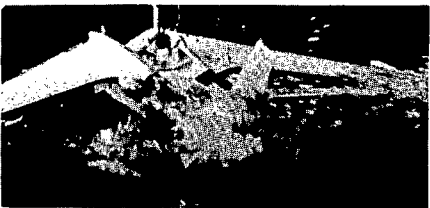
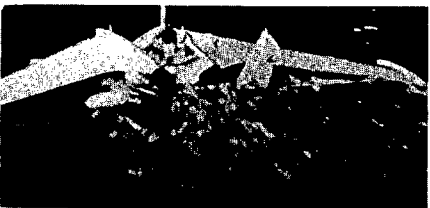
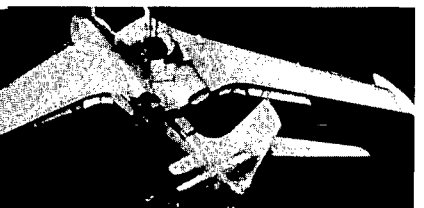


Figure 33.- Main spray envelopes. Power on; Δ_0 , 130,000 pounds; δ_f , 20° ; δ_e , -10° ; center-of-gravity location, 28 percent mean aerodynamic chord.



Time, 0 sec

 $\frac{1}{16}$ sec $\frac{5}{16}$ sec $1\frac{1}{4}$ sec $\frac{9}{16}$ sec $1\frac{1}{2}$ sec $\frac{11}{16}$ sec $1\frac{3}{4}$ sec $\frac{7}{8}$ sec

Damaged elevator



L-68418

Figure 34.- Spray damaging elevator during landing in waves 8 feet high and 255 feet long. Power off; Δ_0 , 110,000 pounds; δ_F , 50° ; center-of-gravity location, 28 percent mean aerodynamic chord.



Time, 0 sec

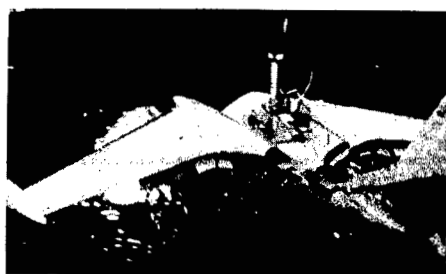
 $\frac{5}{8}$ sec $\frac{1}{8}$ sec $\frac{3}{4}$ sec $\frac{1}{4}$ sec

1 sec

 $\frac{3}{8}$ sec $1\frac{1}{4}$ sec $\frac{1}{2}$ sec $1\frac{1}{2}$ sec

L-68419

Figure 35.- Spray entering air intake during landing in waves 8 feet high and 204 feet long. Power off; Δ_0 , 110,000 pounds; δ_f , 50° ; center-of-gravity location, 28 percent mean aerodynamic chord.



Time, 0 sec

 $\frac{11}{16}$ sec $\frac{3}{16}$ sec $\frac{15}{16}$ sec $\frac{5}{16}$ sec $\frac{13}{16}$ sec $\frac{7}{16}$ sec $\frac{15}{16}$ sec

L-68420

Figure 36.- Spray entering air intake during landing in waves 8 feet high and 204 feet long. Power off; Δ_0 , 110,000 pounds; δ_f , 50° ; center-of-gravity location, 28 percent mean aerodynamic chord.

CONFIDENTIAL

CONFIDENTIAL

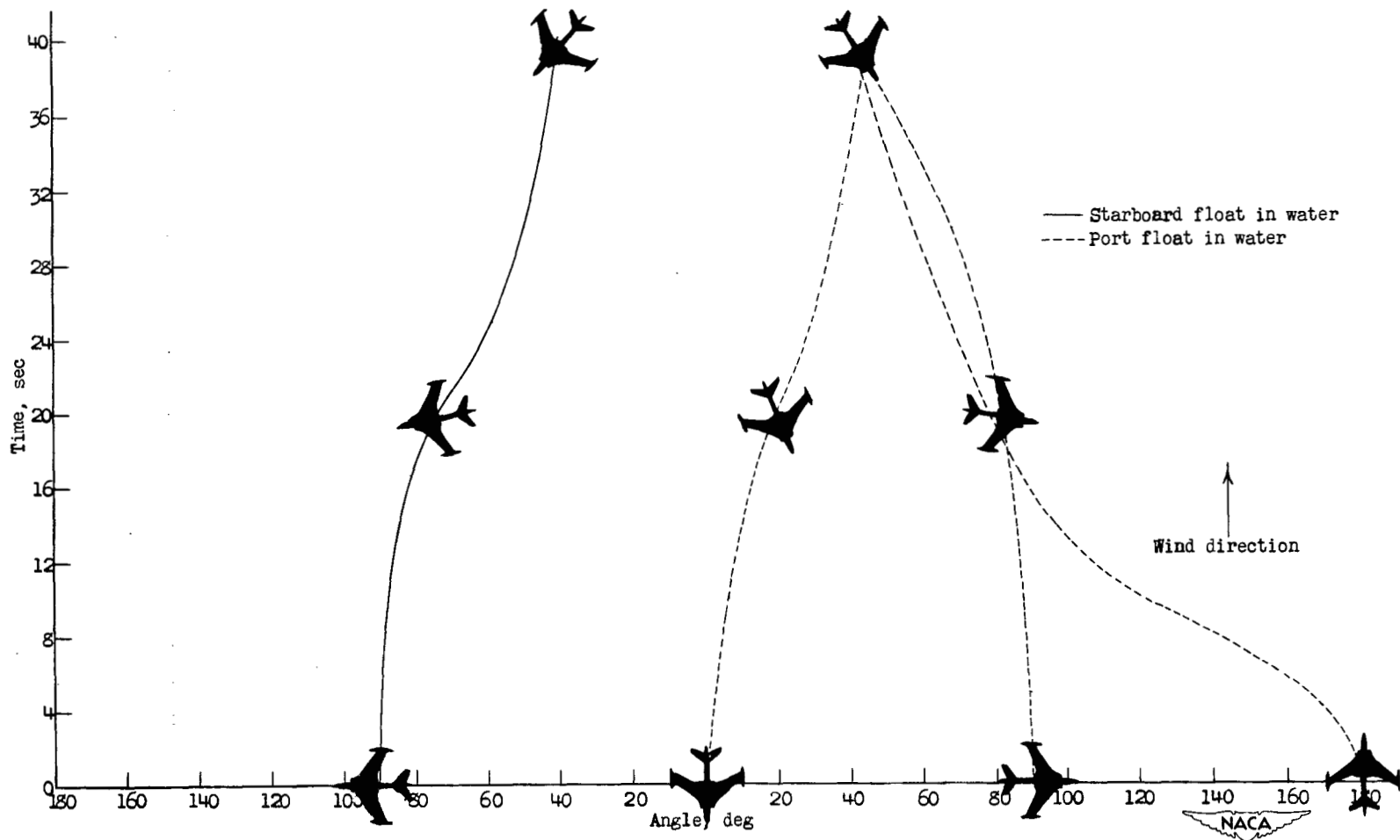


Figure 37.- Drifting characteristics. Δ_0 , 62,000 pounds; center-of-gravity location, 28 percent mean aerodynamic chord; wing velocity, 45 knots.

NASA Technical Library



3 1176 01438 5083